SOME DESIGN ASPECTS OF A DELTA WING IN SUPERSONIC FLOW

By
RAJENDRA KUMAR BERA

DEPARTMENT OF AERONAUTICAL ENGINEERING
INDIAN INSTITUTE OF TECHNOLOGY KANPUR
AUGUST 1973

SOME DESIGN ASPECTS OF A DELTA WING IN SUPERSONIC FLOW

A Thesis Submitted
In Partial Fulfilment of the Requirements
for the Degree of
DOCTOR OF PHILOSOPHY

By
RAJENDRA KUMAR BERA

to the

DEPARTMENT OF AERONAUTICAL ENGINEERING
INDIAN INSTITUTE OF TECHNOLOGY KANPUR
AUGUST 1973

AE-1973-D-BER-SOM

CERTIFICATE

Certified that this work 'Some Design Aspects of a Delta Wing in Supersonic Flow' has been carried out under my supervision and that this has not been submitted elsewhere for a degree.

S. M. Ramachandra

S.M. Ramachandra
Professor, Department of
Aeronautical Engineering
Indian Institute of Technology
Kanpur.

ACKNOWLEDGEMENTS

It is difficult to express in words my sincere gratitude to Dr. S.M. Ramachandra who has been both a teacher and a friend, and without whose patience, understanding and affection this work would not have been possible. I shall always remember the day he suggested the outlines of the work embodied in this dissertation and the advice, encouragement and freedom he has given me in pursuing this subject. To no less a degree am I indebted to his most gracious wife, Leela who always made me feel a part of their family, especially so during the last year and half of this work when I was away from home.

I have been most fortunate in that my parents have spared no efforts, and who even under very trying circumstances, have encouraged me to complete this task. To my mother specially, whose sole concern has been my happiness in whatever I do.

It is a pleasure to thank Dr. S.R. Valluri, Director, NAL, Bangalore, for his interest in this work. His encouragement has been a source of strength to me while I was working as a scientist in the Laboratory.

I gratefully acknowledge the financial assistance from IIT/Kanpur during August, 1969 to September, 1970 and a senior fellowship from the Ministry of Defence, Government of India for the period October, 1970 to November, 1971.

The assistance of the members of the Computer Centres of IIT/Kanpur and IISc/Bangalore is greatly appreciated.

And finally, to my numerous friends at IIT/Kanpur and NAL/Bangalore, each of whom have helped in their own way, my heartfelt appreciations.

CONTENTS

CONTENTS (Contd.)

ABSTRACT

This dissertation looks into the problem of conically cambered delta wings with subsonic leading edges in a steady supersonic stream. The superiority of subsonic over supersonic leading edges has long been recognised because of its favourable leading edge suction which alleviates drag. This provided the motivation for obtaining analytical solutions for the indirect lifting problem by choosing a twist distribution function which is a polynomial of even ordered terms of the conical variable. Thus, wing shapes cambered in a plane perpendicular to the free-stream are easy to visualise and definite trends in the results may be established.

Considerable attention is paid to the problem of obtaining minimum drag shapes subject to a given lift and other equality and inequality constraints. In order to avoid flow separation at the leading edges, the attachment lines were fixed there.

A noted contribution of this dissertation is the use of mathematical programming techniques to formulate the minimum drag problem subjected to realistic constraints which may quite often be stated as inequality constraints. For programming methods, it is shown that orthogonal loadings, as defined by Graham, play an important role in obtaining a simplified formulation. It has also been possible to generalise some drag reduction theorems already known in the literature.

The off-design condition, when leading edge vortices are observed if the wing is slender and the leading edges are subsonic, is studied theoretically. A hybrid method is proposed which uses Polhamus' leading edge suction analogy and a modified Kuchemann-Squire formulation and the problem is solved as a minimum drag problem. Reasonably good agreement at low aspect ratios with available experimental data is observed.

NOMENCLATURE

a	$(M^2-1)^{1/2}\tan\delta$, slenderness parameter
AR	Aspect ratio
b	Wing semi-span
$B(x,y)$	Beta function with arguments x and y
C	A constant, a factor proportional to strength of singularity, Eq. (2.11)
C_l	Two dimensional lift coefficient
C_p	Pressure coefficient
C_r	Root chord
C_o	C/U
C_D	Drag coefficient
C_L	Lift coefficient
C_M	Pitching moment coefficient
$C(\eta)$	Spanwise chord distribution
$\mathcal{C}(\eta)$	Spanwise distribution of load
d_{ij}	The integral $-\int_0^1 L_{2i}(\eta)\, w_{2j}(\eta)\, d\eta$
D	Drag
e	Efficiency factor, π AR C_D/C_L^2
$E(x)$	Elliptic integral of second kind with argument x
$F(\alpha,\beta,\gamma,\delta)$	Hypergeometric function with arguments $\alpha,\beta,\gamma,\delta$
G_{2k}	The integral $\int_0^1 (1-\eta^2)^{\eta_2}\,\eta^{2k}\,d\eta$
$I_{2k}(\eta)$	The integral $\frac{2\sqrt{1-\eta^2}}{2k+1}\int_0^1 \frac{\eta_i}{(\eta_i^2-\eta^2)\sqrt{1-\eta_i^2}}\,d\eta_i$

NOMENCLATURE (Contd.)

J_{2k}	Binomial coefficients in the expansion of $(1-x^2)^{-1/2}$
k	$(1-a^2)^{1/2}$
$K(x)$	Elliptic integral of the first kind with argument x
l_i	The integral $\int_0^1 L_{2i}(\eta)\,d\eta$
$L_{2k}(\eta)$	Pressure distribution due to basic twist distribution $\eta^{2k}/2k$
$L(\eta)$	Total pressure distribution
L	Lift
$L_v(\eta)$	Pressure distribution due to leading edge vortex
M	Pitching moment, free stream Mach number
$Q_{2k}(\eta)$	The integral $\int_\eta^1 \frac{I_{2k}}{\eta_i^2}\,d\eta_i$
$R_{2k}(a)$	The integral $\int_0^1 \eta^{2k}\sqrt{\frac{1-\eta^2}{1-a^2\eta^2}}\,d\eta$
s	Local semi-span
$S_{2k}(a)$	The integral $\int_0^1 \eta^{2k}\sqrt{\frac{1-a^2\eta^2}{1-\eta^2}}\,d\eta$
$T_{2k}(a)$	The integral $\int_0^1 \eta^{2k}\,d\eta/\left(\sqrt{1-a^2\eta^2}\sqrt{1-\eta^2}\right)$
u,v,w	The perturbation velocity components
U	Free-stream velocity
U,V,W	Analytic functions whose real parts are u,v,w
x,y,z	Cartesian coordinates
$z(x,y)$	Wing ordinate distribution

NOMENCLATURE (Contd.)

Special Notations

$\tilde{p}, \tilde{\alpha}$	Pressure and angle of attack distribution respectively in reverse flow with $\tilde{p} = p$
$\underset{\sim}{p}, \underset{\sim}{\alpha}$	Orthogonal pressure and angle of attack distribution respectively

Greek Notations

α	Angle of attack
δ	Wing semi-apex angle
ϵ_{2k}	Constants associated with the twist distributions $\eta^{2k}/2k$
η	Conical coordinate, y/s(x)
λ_i	Lagrange multipliers
ϕ	Perturbation velocity potential
Σ	Summation sign

LIST OF FIGURES

LIST OF TABLES

CHAPTER 1

INTRODUCTION

1.1 General Remarks

Delta wings have frequently found applications in the design of supersonic airplanes because of its ease in manufacture, high wing thickness near the root chord even for small thickness-chord ratios and greater structural rigidity. Fortunately, it is also a planform suitable for theoretical analysis and has been widely studied.

This dissertation studies the analysis of a delta wing, with subsonic leading edges, flying at supersonic Mach numbers and having a conical twist distribution. The superiority of subsonic over supersonic leading edges for such wings has long been recognised because of its favourable leading edge suction which reduces drag. Further, any delta wing must pass through a Mach number range in supersonic flight for which the leading edge is subsonic. The problem, therefore, is of practical interest.

Conical camber was chosen because, within this framework, it is possible to obtain closed form solutions without requiring the wing to be slender. Both the direct and the indirect problems have been attempted in the literature. We have chosen to solve the indirect lifting problem by specifying the twist distribution in even powers of the conical

coordinate.

Since wing shapes of minimum drag are of considerable practical importance, studies have been made using combinations of these twist distributions. In the literature minimum drag wings have generally been obtained for a given total lift and, sometimes, for a given pitching moment. These constraints have always appeared in equality form. The procedure is extended to include both equality and inequality constraints by using the powerful techniques of mathematical programming. In the process the usefulness of orthogonal loadings[32] is shown.

As a corollary to this work it was possible to generalise some of the existing, drag minimization theorems by relating the forward and reverse flows. These theorems, it is felt, should be of help in not only identifying minimum drag shapes but also in obtaining wings with low lift dependent drag.

At off-design conditions, if the wing is slender, with sharp leading edges which are subsonic, leading edge vortices give rise to additional lift which is a non-linear function of the incidence. A new theoretical model which uses Polhamus' suction analogy[56] and a modified version of the Kuchemann[54], Squire[55] formulation is used and the problem solved as a drag minimization problem to predict the pressure distribution. Agreement with available experimental data is good.

1.2 General Review of Supersonic Wing Theory

Conventional airfoil shapes fortunately allow us to linearize the equations of motion and to simplify the boundary conditions. Inspite of this, the problem of a finite wing in subsonic flow has been quite difficult. The case of supersonic flow has been quite encouraging and in several instances have given closed form solutions.

As one moves from the subsonic to the supersonic case, a distinct change in the character of the disturbance field takes place. The fore and aft symmetry of the subsonic flow disappears and the disturbances are limited to the region behind the wing bounded by Mach cones. Because of this asymmetry in the flow all outgoing disturbances result in a drag, called the wave drag, so that even the thickness of a wing or body creates a drag in addition to the drag associated with lift. Thus the drag arising from the lift may be identified partly as vortex drag and partly as wave drag, though both effects are due to the rearward tilt of the lift vector. The vortex drag, which in subsonic flow is also known as the induced drag, may be calculated from considerations of the vorticity in the wake, and depends solely on the spanwise distribution of lift. The wave drag appears due to the energy required to extend the wave system emanating from the wing to infinity.

Hayes[20] showed that at great distances behind the wing, the wave disturbance is concentrated in the vicinity of the Mach

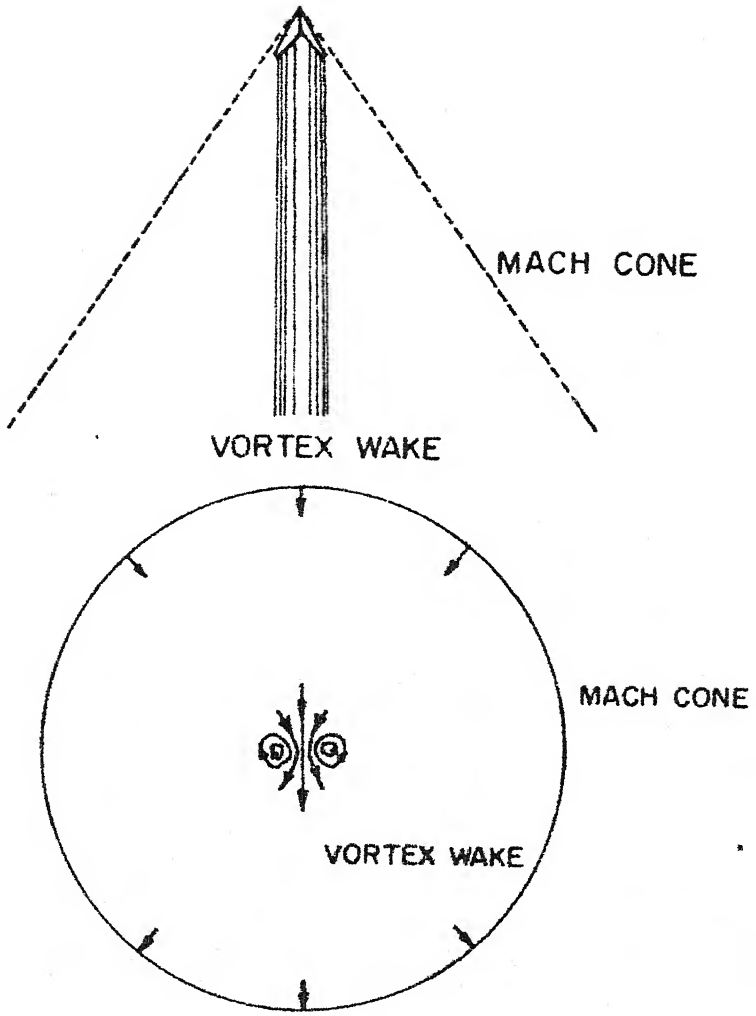

FIG. I.I. DISTURBANCE PRODUCED BY WING AT SUPERSONIC SPEEDS.

cone and does not modify the purely subsonic field of disturbance in the vicinity of the vortex wake, which occupies a relatively small region near the centre of the cone, Figure 1.1. Hence the wave drag and the vortex drag may be separated if calculations are made on the basis of the momentum of the flow at a large distance behind the wing. Alternately, the sum of the wave and the vortex drag or the drag due to lift, may be calculated by integrating the product of the local pressure with the local angle of attack over the entire wing surface.

Using the latter approach it can readily be shown that the drag due to thickness is directly proportional to the square of the thickness-chord ratio, and the drag due to lift is proportional to the square of the lift coefficient. In the linearized theory, it can be further shown that the drag due to thickness and lift are additive and hence the two problems can be treated independently.

Important distinctions arise between cases where the velocity component normal to an edge is subsonic or supersonic. The edges are then known as subsonic or supersonic edges respectively. For a lifting wing with a subsonic leading edge, the flows on the upper and lower surfaces near the edge are no longer independent. The fluid flows around the edge with subsonic velocity, and one obtains a leading edge suction. Furthermore, in the sector enclosed between the leading edge

and the limiting Mach line, the pressure resulting from the upper and lower half spaces must be balanced. In the case of a subsonic trailing edge, the Kutta condition must be satisfied.

In the case of a supersonic leading edge, the flow will be locally similar to an Ackeret flow, provided the edge is sharp. There will be no flow around the edge and the surface of the airfoil divides the flow into independent upper and lower regions. It is also no longer necessary to distinguish between pressures arising from lift and those arising from thickness. The pressure on each surface being determined by the shape of that surface alone.

In the case of a supersonic trailing edge, since disturbances downstream of the trailing edge cannot propagate upstream, the independent pressures on the upper and lower surfaces will be maintained upto a point so near the trailing edge that equalization of the pressure takes place through the boundary layer somewhat gradually. However, in inviscid, linearized theory, it is considered sufficient to let the lift fall to zero behind the trailing edge through an attached oblique shock.

The case when both the leading and trailing edges are supersonic is the simplest to solve, since the flows on the top and bottom surfaces are completely independent and the lifting and thickness problems may be treated in the same

fashion. This is done by representing the surface by a distribution of supersonic sources, a concept first introduced by von Karman and Moore for axisymetric bodies and later extended to wings by Puckett[22]. In the linearized theory it was shown that the local source strength is proportional to the local angle of attack or the streamwise slope. The calculation for the pressure distribution then reduces to integrating a double integral rather than solving an integral equation.

The problem of partially subsonic leading edges was elegantly solved, apparently independently, by Evvard[24] and Krasilchikova[25]. The method requires at least some part of the leading edge to be supersonic. In their method, to obtain the pressure at a point, it was necessary to integrate over the shaded region only and completely ignore the unshaded regions, Figure 1.2. The method was used by Etkin and Woodward[26] to obtain an approximate solution for a flat delta wing with subsonic leading edges. They also gave a procedure for arbitrary downwash distributions. For the case of a plane delta wing, it was shown by comparison with exact solutions, the error incurred by neglecting the contributions after the third reflection, is negligible.

For sharp subsonic leading edges, the attached flow theory predicts either infinite or zero load at the edges. Because of the tendency of the flow to separate with the

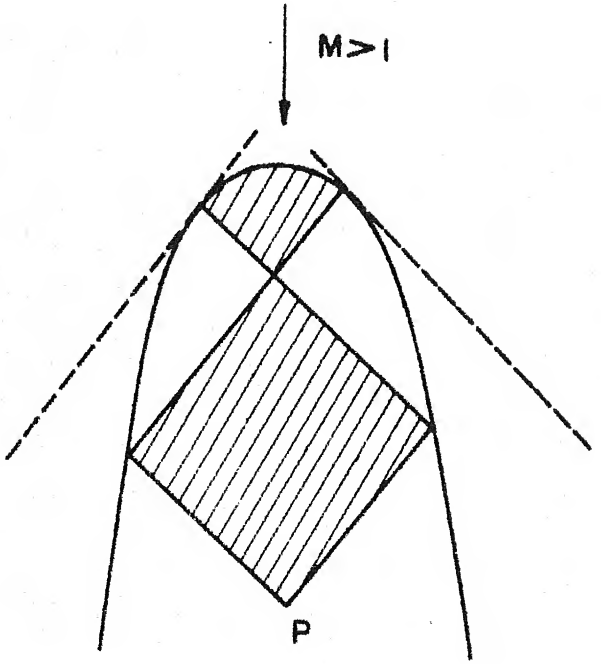

FIG. 1.2a. EVVARD-KRASILCHIKOVA METHOD

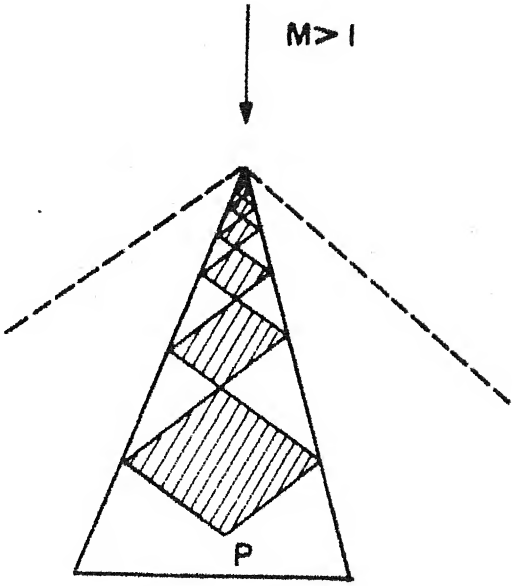

FIG. 1.2b. ETKIN-WOODWARD METHOD

infinite type of load at the leading edge, it is more useful to consider load distributions of the latter type. There is evidence that wings with drooped edges sustain to a greater degree, the theoretical value of suction than plane wings[63]. Thus, cambered wings may be expected to be better than plane wings from this view point. In what follows, we discuss cases of attached flow and zero load along the leading edges at the design conditions unless otherwise specified.

1.3 Conical Wing Theory

The problem of wings of arbitrary planform with completely subsonic leading edges has generally not been solved. The flat delta wing with subsonic edges has been solved approximately by Etkin and Woodward[26] as mentioned earlier. However, more elegant and closed form solutions for the delta wing have been obtained using conical flow theory originally due to Busemann[1]. Conical flow is defined as a flow field in which all the velocity components, and hence the pressure and slope of streamlines, are constant along rays emanating from a point (the wing apex in this case). Conical camber is the name given to that distribution of angle of attack which produces conical flow over a wing surface. With this restriction, the three dimensional Prandtl-Glauert equation can be reduced to a two dimensional Laplace equation and the well developed method of complex variables may be used.

Early investigators using conical flow assumptions also made the low aspect ratio assumption thereby rendering their solutions independent of Mach number and devoid of the wave drag. Both the direct and the indirect lifting problems were studied. Probably the earliest of such attempts was that of Jones[4] which resulted in his famous low aspect ratio theory and gave a simple and elegant analytical solution. Under similar assumptions Shaw[10] in his studies of leading edge controls on a delta wing gave the solution for the case when the central portion of the wing is straight and the outboard portion drooped. The downwash distribution in his case was of the form

$$w/U = a, \qquad 0 \leq |\eta| \leq \bar{\eta}$$

$$= a + b(\eta - \bar{\eta})^n; \quad \bar{\eta} < |\eta| \leq 1$$

where n = 0, and w is the z-perturbation velocity, U the free-stream velocity, η the conical coordinate, a, b, n and $\bar{\eta}$ are constants. The work was extended by Brebner[2] for the cases n = 1 and 2 and by Weber[9], who in addition, considered the constant a, b and $\bar{\eta}$ as functions of the streamwise coordinate, x. She was, therefore, able to extend the method to cases of arbitrary planform and downwash distribution for very slender wings. However, this kind of extension is implicit in any low aspect ratio theory as given by Jones. Further, the basic low aspect ratio solutions are conical.

In the above work,[2,4,9,10] the boundary condition on the wing surface was satisfied on an auxiliary plane, usually the plane $z = 0$. Using the above assumptions but with the surface boundary condition being satisfied on the wing camber surface, Smith[5] solved for the case when the spanwise camber line is a circular arc. Cooke[3], in the same spirit, extended it to the case when the camber line has a straight central portion with drooped edges, a configuration obtained by starting from a circle through several transformations originally due to Maskell. Smith's results come out as a special case.

The direct problem of specifying the load distribution and determining the spanwise camber was solved by Smith and Mangler[6], again using the low aspect ratio assumption and satisfying the surface boundary condition on the plane $z = 0$. They could relate the twist distribution for different values of the slenderness parameter, but carrying the same spanwise distribution of load, and hence considerable attention was paid to the slender wing solution. In particular, it was shown that for slender wings, the camber could be designed to give lift dependent drag factors as close to unity - the theoretical minimum for wings shedding substantially plane vortex sheets - as one wished. Thus, a wing cambered to have an attachment line along the leading edge at its design C_l could be expected to show a useful reduction

in lift dependent drag compared with the sharp edged uncambered wing, having at all $C_L \neq 0$, separation at the leading edge.

A not very useful feature of Smith and Mangler's work is the wavy camber shapes that result due to the representation of the potential function by an infinite series. As the number of terms increases in the series, the lift dependent drag factor decreases and the camber line contains more, but less pronounced, waves. A chordwise waveiness in the pressure distribution gives rise to the undesirable feature of having several compressions on the wing.

The low aspect ratio assumption appears to give reasonable results when applied to delta wings in supersonic flow. For example, it predicts the pressures near the apex of a plane delta wing with good accuracy and the shapes of the spanwise pressure distribution are generally in good qualitative agreement with experimental results, although errors in scale exist which increase as the trailing edge is approached[67]. However, the low aspect ratio assumptions do not distinguish between subsonic and supersonic speeds. In the subsonic range the theory fails to account for the Kutta condition at the trailing edge and causes an overestimation of the pressures on the rear part of the wing which gives rise to large errors in the lift and pitching moment.

The low aspect ratio theory when applied to plane non-delta planforms at incidence shows that the lift depends on the increase in width of the sections in a downstream direction. The sections behind the section of maximum width develop no lift. Further, the spanwise loading is independent of the planform and depends not on the area but on the width of the wing. A rectangular planform would thus have all the lift concentrated at the leading edge.

The delta wing problem, without the low aspect ratio assumption, has been attempted among others by Baldwin[13], Tsien[5], Holla[7] and in the present work. The first two specify the pressure distribution as an infinite series of certain pressure functions and solve for the camber shape. The work of Holla and the present dissertation specify the twist distribution and solve for the pressure distribution.

Tsien's work showed that when a finite number of terms in the solution are taken, $(Z/x)_{opt.}$ for the minimum drag shape, has an infinite value at the centreline. This undesirable feature may be avoided by adjusting the appropriate constants so that the terms contributing to this feature are zero. By doing so it was found that the increase in $(C_D/C_L^2)_{opt}$ was negligible. This is not surprising, as the central part of the wing shape acts like a fin with very small effect on the pressure distribution. Tsien carried out the analysis for both full leading edge and no leading

edge suction. For the suction case he found the minimum C_D to be almost identical to the plane wing at the same C_L except when the leading edge lies close to the Mach cone when noticeable improvements of about 8% in C_D/C_L^2 over the flat plate with suction is obtained. The suction case is not of great importance since in practice it is difficult to realise its full value due to separation.

The no-suction case shows appreciable improvement over that of the corresponding flat plate. In fact, the minimum C_D is only slightly higher than the minimum of the suction case. The use of conical camber will almost entirely overcome the unfavourable effect of the loss of suction force.

The indirect problem was considered by Holla[7] wherein he used conical twist distributions of the type $(1-a^2\eta^2)^{3/2}\eta^{2n}$ for n=1 to 5, where a is the slenderness parameter and η the conical coordinate, and obtained the corresponding pressure distributions. He also arrived at similar conclusions regarding minimum drag as those of Tsien. It was found in this work and in all the others mentioned earlier, that in the no-suction case, reduction in drag is obtained by drooping the outboard portion of the wing so that the pressures acting on that part give rise to a thrust component. The present work considers twist distributions of the type η^{2n} for positive integral values of n. The pressure distributions are obtained in a series solution in increasing powers of the

slenderness parameter, a. These results are subsequently used to obtain minimum drag wings under equality and inequality constraints.

An obvious extension to conical flows would be cases where the velocity components vary according to some power of x, y and z along each ray. Such flows are called quasi-conical flows and its velocity potential is described by homogeneous functions of the coordinates x,y and z and contain the conical flow field as a special class of degree zero. The quasi-conical flows, because of lesser restriction on the flow properties would naturally give rise to minimum drag wings that are aerodynamically more efficient compared to conical wings. However, the mathematical problem is considerably more complicated. Lance[11,12] among others has utilised this method to find the properties of wings arrived at by using the first few terms of a certain quasi-conical series for the downwash distribution. These results, along with the conical flow results of this dissertation, may be used to find the wave properties by using the lift cancellation method and also to obtain aerodynamically efficient wings.

Some experimental results on conical wings are reported in reference 62 and 63. In reference 63, wings are designed using Brebner's twist distribution for a delta wing of 30 degree semivertex angle and a spanwise elliptic thickness distribution. The corresponding plane delta wing is reported

in reference 62. The results show the possibility of obtaining a theoretical zero load condition along the leading edge (at a slightly higher incidence than theoretically predicted). At incidences below the designed value, separation on the lower surface is suppressed while the development of a turbulent boundary layer delays separation on the top surface. Comparison between plane and cambered wings show that both have the same lift curve slope and nearly equal drag at the design incidence.

In another set of experiments[64] on a plane, a biconvex and a conical delta wing of semiapex angle 37.5 degree it was found that spanwise cambered wings with drooped leading edges achieve higher leading edge suction than a plane wing, specially at high subsonic and transonic speeds. The suction peak at the leading edge of a plane delta wing is replaced by a region of finite suction over the forward facing area by the introduction of spanwise camber. The modified pressure distribution helps flow attachment at the leading edges at higher incidences.

1.4 Drag Minimization

One of the central problems in aerodynamics is the determination of minimum drag wing shapes for a given planform and given lift. For delta and delta type wings it was shown that twist plays a more important role than camber[32].

In this respect conical camber may be considered to give useful drag reductions. It was again shown by Tsien[5] that superposing a parabolic camber on a conically cambered wing gave additional relief in drag. Cohen[34] using the quasi-conical results of Lance[11,12] obtained lower values of drag compared to certain conical shapes but some of her wings have upturned leading edges which are prone to flow separation in a viscous medium. It is also not certain that all low drag wings obtained by using the linearized potential flow theory will show similar reductions in drag in a real fluid.

What is then required is that in the absence of an adequate viscous theory, the potential flow theory be used to assimilate realistic design criteria by introducing quantitative and qualitative information, some of which may have nothing to do with aerodynamics, into the minimum drag problem. It may, for instance, be desirable to have a cambered centre section of the wing so that, at the design C_L, its incidence is smaller than for the uncambered centre section with the same slope at the trailing edge of the wing and thus possibly decrease the height of the undercarriage. It would certainly be desirable to avoid upturned leading edges as in Cohen's design. It might also be useful to have a monotonically decreasing incidence from the wing root to the tip for favourable stalling characteristics. From a manufacturing point of view it might be useful to have a straight spanwise central portion

and a different contour in the outboard region. Or the wing may be required to follow a certain given contour over some part of the wing.

Clearly, these problems will arise in practice and the present theoretical design methods are not adequate. However, under restricted conditions several important results in drag minimization are available in the linearized theory. Thus, it is shown that the induced drag is a minimum in subsonic flow if the spanwise distribution of lift is elliptic. The induced drag, even otherwise, is independent of the details of the chordwise pressure distribution. Subsequently, Munk[29] showed that the drag due to lift is a minimum if the downwash in the combined flow field is a constant. The combined flow field is the field obtained by superimposing the flow fields due to the wing in forward and in reverse flows. Again, it was shown by Jones[30,31] that the drag is a minimum for a given volume if the pressure gradient in the free-stream direction is a constant, and for a given maximum thickness if the pressure is constant in regions forward and aft of the maximum thickness. One notices that these results help us to identify minimum drag shapes. However, except under very simple circumstances, they do not tell us what the minimum value of the drag is or how to achieve it. The combined flow field results are valid for both subsonic and supersonic speeds. The utility of the combined flow field

is that it reduces a three dimensional subsonic flow problem to a two-dimensional one and, in general, simplifies the calculations in the three dimensional supersonic case.

A method which has considerable design value was given by Graham[32] using the concept of orthogonal loadings, defined as loadings whose mutual interference drag is zero. Thus, along with the velocity components, pressures, etc., the drag is also superposable in the linearized theory. Graham further showed that two orthogonal loadings, each carrying positive lift, when combined in any fashion to support a given total lift, will give lesser drag than either load supporting the same total lift.

The most common procedure, by far, in designing minimum drag wings has been to use the classical Lagrange multiplier method. Thus Tsien[8], Smith and Mangler[6], Nolla[7], Grant[66], Cohen[34] and many others have used it to design conical or other types of wings for a given lift constraint. The results of the combined flow field have generally not been of great help and we are aware of only one application where Ginzel and Multhopp[35] have used the constant downwash result to design wings in supersonic flows. The orthogonal loading method was used by Graham[32] and his coworkers[33] for some simple shapes. It has also been used in this dissertation.

The linearized theory provides some interesting theorems relating the forward and reverse flows, which are

generally referred to as the flow reversal theorems. Thus, Munk[29] showed that for a given lift distribution in subsonic, steady flow the drag is unchanged by reversal of flow direction. Kármán[21] and Hayes[20] showed this to be valid for the supersonic case also. Several more theorems relating the lift curve slope, etc. were derived by others and finally they were systematized by Ursell and Ward[36] and Flax[37-39] which also account for the leading edge suction, if any. The theorem is stated simply as

$$\int p_F \alpha_R \, dA = \int p_R \alpha_F \, dA \qquad (1.1)$$

where p and α are the pressure and angle of attack distributions and the subscripts F and R refer to forward and reverse flows. The integration is over the entire wing planform. This result is valid for both steady and unsteady flows, at subsonic and supersonic speeds, subject to the requirement that the Kutta condition is satisfied at subsonic trailing edges whenever they appear.

Using the above mentioned results, generalizations of some existing theorems are presented in Chapter 4, which should be of assistance in designing low drag wings. Also, the relatively unused but nevertheless powerful methods of mathematical programming (MP) have been adopted for designing minimum drag wings under realistic constraints (which can often be stated as a set of inequality constraints). Chapter 6

is completely devoted to this aspect. In Chapter 5 the method of orthogonal loadings is placed on a more formal footing and its importance in formulating the minimum drag problem as a VP problem is shown. The different methods are compared in Chapter 7.

1.5 Leading Edge Vortex Phenomenon

The low aspect ratio plane delta wing, which has a small lift-curve slope, must operate at high angles of attack at low speeds to sustain a given lift. However, even at moderate incidences, the flow at the leading edges separate. The boundary layers on the outer parts of the upper and lower surfaces flow outwards towards the leading edge and there coalese, forming free shear layers. If the leading edges are sharp, the primary separation is fixed along them. On a delta or a delta type wing, a single shear layer forms at each leading edge, and assumes under the influence of its own voticity, the form of a spiral vortex which lies above the wing. This spiral vortex exerts considerable influence on the pressure distribution. The oncoming flow bends the vortex sheet down and reattaches it to the wing surface. The oncoming flow in the inboard region of this attachment line moves directly downstream, while the boundary layer which originates outboard of the attachment line encounters a steep pressure rise as it passes outwards under the vortex towards the leading edge and separates thus originating a

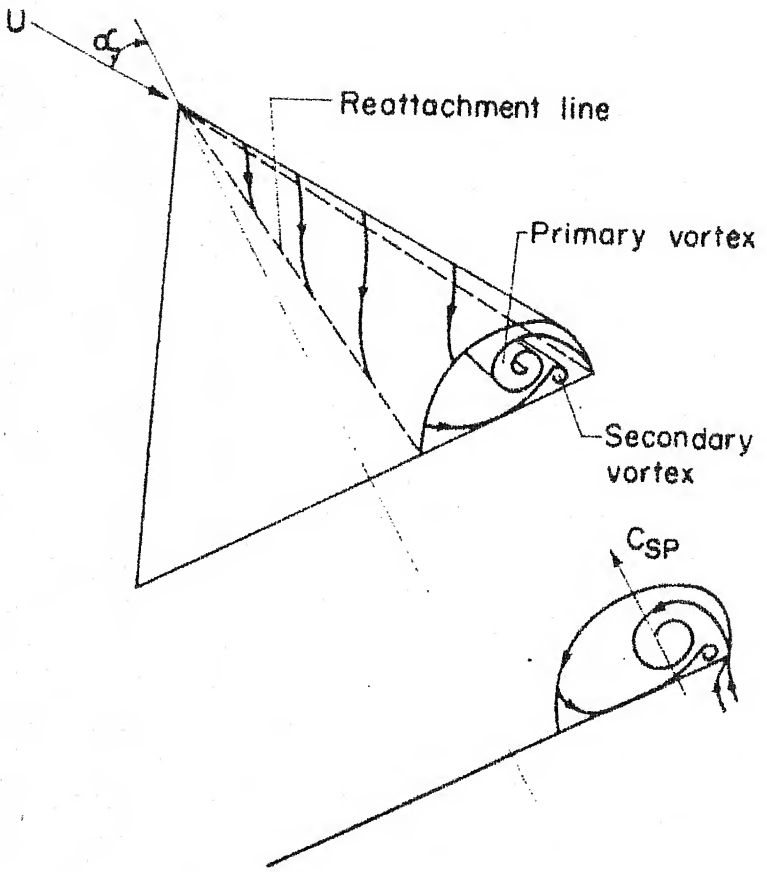

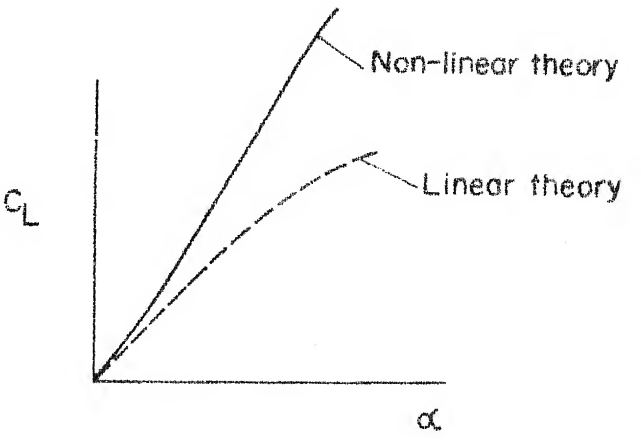

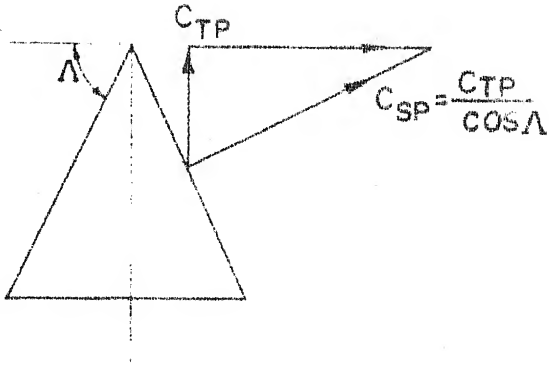

FIG. 1.3 LEADING EDGE VORTEX

second shear layer, Figure 1.3. The scale of this secondary separation is small and has been neglected in all theoretical analysis put forward so far. This type of flow is found at subsonic speeds when the sweepback of the leading edges is about 60 degrees or more. A similar situation occurs at supersonic speeds when the leading edges are subsonic, the flow reattaching with increase in Mach number[55].

The leading edge phenomenon has attracted a great deal of attention in recent years because only one type of stable flow can be maintained over a wide range of attitudes and Mach numbers without the need for flow control devices. The phenomenon is associated with substantial increases in the lift and the lift-curve slope, both of which tend to reduce the need for high lift devices and high incidences during take-off and landing. This mode of separation is different from the conventional boundary layer separation in the sense that in this case the increase in drag is not prohibitively high as in the case of boundary layer separation. The leading edge vortex phenomenon is thus an attractive substitute for high lift devices.

The phenomenon is undoubtedly due to viscosity which plays an important role in the boundary layers on the wing surface, in the initial development of the free shear layers and in a small sub-core which is found in the centre of the spiral vortex. The viscous sub-core is typically no more than

5% of the diameter of the vortex[45] and may have axial velocities two to three times the free stream value. Earnshaw's[43] detailed investigations show that the total pressure in the core of the vortex is considerably lower than the surrounding stream and has its minimum value at the vortex centre.[46] This fact may be used to experimentally determine the vortex centre. Outside of these regions the flow field appears to depend little on the Reynolds number and the flow may be assumed to be inviscid.

Due to separation, the pressure peaks indicated by the attached flow theory are not developed, but peaks are developed inboard of the leading edges. Experimentally it has been observed for delta wings that the longitudinal centre of the leading edge suction, the potential flow aerodynamic centre, and the aerodynamic centre with leading edge vortex are approximately the same. It would thus appear that the redistribution of the potential flow part of total lift is primarily spanwise.

Kirkpatrick's[47] experiments showed that the path traced by the vortex centre above a wing as its incidence is increased is significantly affected by the dihedral angle of the wing, and becomes more curved and closer to the η-axis as the dihedral is increased. Further, for a rhombic cross-section the vortex centre is closer to the η-axis than for a biconvex cross-section having the same leading edge and dihedral angles.

Also, the normal force coefficient is smaller for rhombic cross-sections than for biconvex cross-sections, and decreases as the dihedral angle increases.

Associated with this is the phenomenon of vortex breakdown first observed by Peckham and Atkinson[46] which can be a limiting factor on the operating attitudes of slender winged aircraft. The possibility of its occurrence in the wake of a large aircraft may be hazardous in dense air traffic. Breakdown may occur earlier over one side of the wing giving rise to unpleasant rolling and pitching motions and loss of lift. This phenomenon is being widely studied both experimentally and theoretically. The theoretical investigations have naturally resorted to viscous flow models. For an excellent review on this topic, one may refer to Hall[10].

The breakdown has been observed in highly swirling flows and seems to require an adverse pressure gradient in the axial direction. Placing an object on the axis of the flow downstream appears to drive the flow further upstream, while a reduction of pressure by suction will move it further downstream and eventually eliminate it altogether. The breakdown surprisingly seems to depend little on the Reynolds number both for laminar and turbulent vortex cores upstream of breakdown. The effect of compressibility seems not to have been studied in detail in the literature.

Several potential flow models have been constructed to predict theoretically the aerodynamic characteristics of the leading edge vortex phenomenon. These may be classified into the following six categories:

1. Cross flow theory - This is an empirical procedure due to Betz[42] based on the assumption that the lateral cross flow of the wing becomes important if the aspect ratio is very small. The non-linear term for the force coefficients results mostly from the drag coefficient of this almost two dimensional cross flow. Calculations are generally based on the cross flow of a rectangular plate with a drag coefficient of 2.0.

2. Bollay-Gersten theory - This type of model was first proposed by Bollay[40] for a very low aspect ratio rectangular wing at the instance of von-Kármán, and comprises a chordwise distribution of constant strength horse-shoe vortices. The vortices are stretched across the span and leave at the side edges. The free vortices are no longer in the plane but shed rearwards at an angle $\alpha/2$, where α is the wing incidence, to the wing surface. Gersten[41] subsequently used this for a delta wing by subdividing it into small rectangular elements and using Truckenbrodt's theory[66] for each of these elements. The non-linear behaviour of C_L with α is predicted quite well and is principally due to the non-planar distribution of vortices.

3. Conical theory - These models use the low aspect ratio assumption by working in the Trefftz plane and the solutions may therefore be considered conical. An attempt is made to represent the physical vortex pattern in this Trefftz plane by placing a concentrated vortex at the core and joining it by an appropriate feeding line to the leading edge. Thus Legendre[48] who pioneered this method, places only two force free point vortices without the feeding line and arrives at non-unique solutions as pointed out by Adams[49]. This model obviously violated the vorticity laws. Brown and Michael[51] modified the solution by connecting the point vortex to the leading edge with a straight feeding line thereby satisfying the vorticity laws. Mangler and Smith[52] use instead a curved feeding line. In these models the strength and position of the core vortex and the feeding line in the Trefftz plane are determined by the boundary conditions that the normal velocities on the wing surface vanish and the leading edge vortex sheets be stream surfaces and sustain no pressure difference. However, the approximations made show a pressure difference across the feeding sheet so long as the isolated vortex continues to grow in strength in the streamwise direction, hence, an integral form of boundary condition is applied, namely, the net force acting on the vortex system must vanish. The results show qualitative agreement but not good quantitative agreement.

4. Kuchemann-Squire theory - Kuchemann[54] and later Squire[55] used a model wherein the vertical displacement of the vortex core was neglected, and the vorticity was assumed concentrated in a thin sheet in the z=0 plane, which is assumed to give a piecewise continuous downwash distribution. Their choice for the downwash was

$$\begin{aligned} w(\eta) &= -\alpha_1, \qquad 0 \le |\eta| \le \eta_0 \\ &= -\alpha_2, \qquad \eta_0 < |\eta| \le 1 \end{aligned} \tag{1.2}$$

where α_1, α_2 and η_0 are constants and η the conical coordinate. Three conditions are needed to evaluate the constants. Two of them are, the load at the leading edge must vanish, and the average downwash must equal the incidence, i.e.

$$\alpha = \alpha_1 + (1-\eta_0)\,\alpha_2 . \tag{1.3}$$

For the third condition Kuchemann assumed a linear variation of η_0 with α, such that $\eta_0 = 1$ for $\alpha = 0$ and $\eta_0 = 0$ for $\alpha = \pi/2$, and solved the problem using the low aspect ratio assumption. Squire removed the low aspect ratio assumption and equated the lift developed by his theory for a = 0 (slender wing) to that of Mangler and Smith[52] as the third condition. For thin wings the results are good.

5. The suction analogy - A thory introduced by Polhamus[56] is based on an intuitive assumption that the normal force on

the upper surface required to maintain the flow about the vortex is the same as the leading edge suction force required to maintain attached flow about the leading edge in the potential flow case. In subsonic flow, this suction force may be calculated using any of the well established lifting surface theories. For plane delta, arrow, and diamond planforms, correlation of C_L vs. α with experiments over a range of subsonic to supersonic Mach numbers is excellent.

6. Maskell's similarity theory - Similarity parameters that relate the vortex development with incidence above slender, conical wings were found by Maskell[69]. Using these the development of the flow field around each of a whole class of slender wings can be predicted, provided the development of the field around one member of the class is determined.

The validity of Maskell's theory was checked against experiments by Kirkpatrick[47] on a number of slender, conical wings with different cross-section shapes, leading edge angles, and dihedral angles at subsonic speeds, which demonstrated to a remarkable degree the validity of Maskell's theory. The position of the vortex core (suitably scaled) was found to be independent of the wing cross-section shape and to depend only on its leading edge angle and a generalised incidence parameter which is a function of the wing geometry. The results are expected to be valid at supersonic speeds also.

In the third chapter we propose a new model which uses the Polhamus' suction analogy and a modified Kuchemann-

Squire approach and pose the problem as a minimum drag problem. The method gives pressure distributions which agree fairly well with experimental results for a plane delta wing.

It may be noted that Carafoli has also attacked the problem in which the thickness of the wing is accounted for. The analysis is quite tedious and lengthy. We have, in keeping with the rest of the literature, neglected the thickness effect and assume that such effects are superposable.

1.6 Concluding Remarks

To summarize, the aerodynamic and geometric properties of conically cambered wings with subsonic leading edges flying at supersonic Mach numbers are given in Chapter 2. Their off-design performance at small and large incidences are given in Chapter 3. The theoretical model proposed for the large incidence case is verified against experimental data for a plane delta wing and is found generally to be in good agreement for low aspect ratios.

The drag minimization theorems are reviewed and extended in Chapter 4 for lifting wings. Chapters 5 to 7 discuss different methods of obtaining minimum drag wings subjected to equality and inequality constraints with the help of orthogonal loadings and the application of mathematical programming.

CHAPTER 2

CONICALLY CAMBERED DELTA WINGS

2.1 Governing Equations

The partial differential equation governing the flow past a thin wing in supersonic flow is given by

$$(M^2-1)\,\phi_{xx} = \phi_{yy} + \phi_{zz} \qquad (2.1)$$

where ϕ is the perturbation velocity potential, M is the free-stream Mach number and (x,y,z) are the cartesian coordinates. Written in cylindrical polar coordinates, we have

$$(M^2-1)\,\phi_{xx} = \phi_{rr} + \frac{1}{r^2}\phi_{\theta\theta} + \frac{1}{r}\phi_r \qquad (2.2)$$

where

$$y = r\cos\theta \quad , \qquad z = r\sin\theta \qquad (2.3)$$

If the flow is conical one may use

$$x/\beta r = \chi \quad , \qquad \beta = \sqrt{M^2-1} \qquad (2.4)$$

and write (2.2) as

$$(\chi^2-1)\,\phi_{\chi\chi} + \phi_{\theta\theta} + \chi\phi_\chi = 0 \qquad (2.5)$$

where $\chi < 1$ characterises the exterior of the Mach cone at the apex and $\chi > 1$ the interior of the Mach cone. If one chooses $\chi = \mathrm{ch}\xi$ for $\chi > 1$, then (2.5) reduces to the Laplace

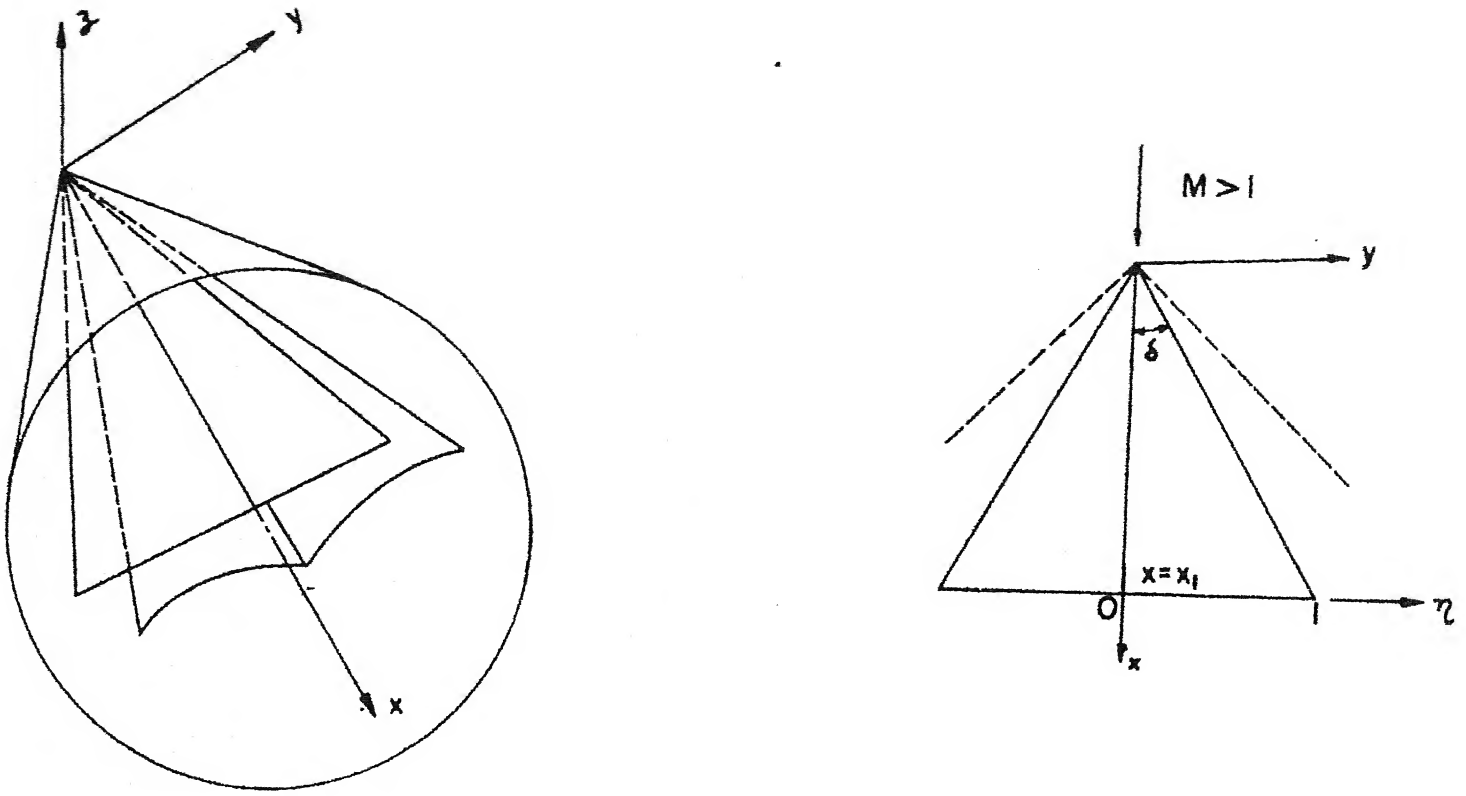

FIG. 2.1. THE WING-MACH CONE SYSTEM

equation valid inside the Mach cone.

$$\phi_{\xi\xi} + \phi_{\theta\theta} = 0 \ . \qquad (2.6)$$

If one chooses $\chi = \cos\eta$ for $\chi < 1$, then (2.5) reduces to the wave equation valid outside the Mach cone.

$$\phi_{\eta\eta} - \phi_{\theta\theta} = 0 \ . \qquad (2.7)$$

Here $\xi = 0$ corresponds to the Mach cone and $\xi = \infty$ the cone axis. $\eta = 0$ corresponds to the Mach cone and $\eta = \pi/2$ the plane $x = 0$. We assume the wing to lie in the region $x \geq 0$, so that $\phi = 0$ for $x < 0$, Figure 2.1.

The region of immediate interest is the wing surface lying inside the Mach cone. The surface condition requires that velocities normal to the surface must vanish. An additional condition is required to blend the flows inside and outside the Mach cone. This is obtained from the fact that "there exists agreement as to $\chi = 1$ for all derivatives of ϕ, defined in the region inside or outside the Mach cone, provided that there is agreement for the function itself[14]". Since disturbances cannot propagate upstream of the Mach cone, it follows that if the free-stream is uniform, the perturbation velocity potential ϕ will be zero on the Mach cone.

To obtain expressions relating the perturbation velocity components u, v, and w, the irrotationality condition

is used which means that

$$x\,du + y\,dv + z\,dw = r\,(\beta\chi\,du + \cos\theta\,dv + \sin\theta\,dw)$$

be an exact differential. This can occur only if this expression is identically equal to zero, with u, v, w being functions of χ and θ. Hence,

$$\beta\chi\,du + \cos\theta\,dv + \sin\theta\,dw = 0 \qquad (2.8)$$

At this stage it is convenient to use complex variables. We, therefore, define

$$\begin{aligned} \zeta &= \theta + i\xi \quad , \quad \bar{\zeta} = \theta - i\xi \\ U(\zeta) &= u(\theta,\xi) + i\bar{u}(\theta,\xi) \\ V(\zeta) &= v(\theta,\xi) + i\bar{v}(\theta,\xi) \\ W(\zeta) &= w(\theta,\xi) + i\bar{w}(\theta,\xi) \end{aligned} \qquad (2.9)$$

where the functions U, V and W are analytic functions of ζ, the real parts of which are the perturbation velocities u, v and w respectively.

With further manipulations between (2.8) and (2.9) the following equations result

$$-\beta\,dU = dV/\cos\zeta = dW/\sin\zeta \qquad (2.10)$$

which are known as the compatibility conditions.

In principle, if the boundary conditions are sufficient to determine either U or W, the remaining components can be

found by integrating. The integration constant is found from the condition on the Mach cone except for an imaginary constant which is of no use to us. The case when $\mathcal{W}$ is given over some regions and u on others is more difficult to solve. A rather complete list of solutions with different kinds of boundary conditions are listed in Jones and Cohen[19].

It is generally convenient to use a conformal representation for studying this problem. For the particular case of a lifting delta wing with subsonic leading edges and at zero yaw, Garafoli derived a relationship between the u and w components of velocity on the wing surface[17].

$$u(\eta) = \frac{U C_0}{\tan\delta \sqrt{1-\eta^2}} + \frac{U}{\pi} \tan\delta \int_0^1 \frac{d\mathcal{W}(\eta_i)}{d\eta_i} \cdot \frac{\eta_i}{\sqrt{1-a^2\eta_i^2}} \times \ln\left[\frac{\sqrt{1-\eta^2}+\sqrt{1-\eta_i^2}}{\sqrt{1-\eta^2}-\sqrt{1-\eta_i^2}}\right] d\eta_i \tag{2.11}$$

and

$$-\mathcal{W}(o) = \frac{C_0 E(k)}{\tan^2\delta} + \frac{2}{\pi} a^2 K(k) \int_0^1 \frac{d\mathcal{W}}{d\eta} \frac{\eta\sqrt{1-\eta^2}}{\sqrt{1-a^2\eta^2}} d\eta + \int_0^1 \frac{d\mathcal{W}}{d\eta} d\eta - \frac{2}{\pi} K(k) \int_0^1 \frac{d\mathcal{W}}{d\eta} \int_0^\phi (1-a^2\sin^2\phi)^{1/2} d\phi\, d\eta + \frac{2}{\pi}\left[K(k)-E(k)\right] \int_0^1 \frac{d\mathcal{W}}{d\eta} \int_0^\phi (1-a^2\sin^2\phi)^{-1/2} d\phi\, d\eta$$

where η is the conical coordinate y/s(x), s(x) is the local semi-span, U the free-stream velocity, $a = \sqrt{M^2-1}\tan\delta$, $k = \sqrt{1-a^2}$, and δ is the semi-apex angle. K and E are elliptic integrals of the first and second kind respectively.

The net pressure coefficient or load at any point is given by

$$L(\eta) = C_p^- - C_p^+ = 4u/U \qquad (2.13)$$

where C_p is the pressure coefficient, + and - refer to the top and bottom surfaces respectively. On substituting for u in (2.13) we have

$$L(\eta) = \frac{4C_0}{\tan\delta\sqrt{1-\eta^2}} + \frac{4\tan\delta}{\pi}\int_0^1 \frac{\eta_i}{\sqrt{1-a^2\eta_i^2}} \ln\left[\frac{\sqrt{1-\eta^2}+\sqrt{1-\eta_i^2}}{\sqrt{1-\eta^2}-\sqrt{1-\eta_i^2}}\right] \times \frac{dw}{d\eta_i}\, d\eta_i . \qquad (2.14)$$

The first term on the right is singular and corresponds to a plane triangular wing. The second term is the load distribution that vanishes at the leading edges. For a given wing and design Mach number, zero load at the leading edge is realised when C_o is zero. This will be so only at one incidence which is given by (2.12).

For arbitrary $w(\eta)$, difficulties arise because of the logarithmic singularity and the term $\sqrt{1-a^2\eta_1^2}$ when a = 1

in the integral. However, closed form solutions are possible for many cases of interest.

2.2 Solutions for Polynomial Twist Distributions

The downwash distribution $w(\eta)$, which we shall henceforth call the twist distribution, used here to solve Eq.(2.14) is is

(2.15)

which to the author's knowledge has not been solved elsewhere. On substituting for $w(\eta)$ and expanding the term $(1-a^2\eta^2)^{-1/2}$ in a binomial series

$$(1-a^2\eta^2)^{-1/2} = \sum_{n=0}^{\infty} J_{2n}\, a^{2n}\, \eta^{2n}, \quad a < 1$$

where

$$J_{2n} = \frac{(2n-1)!!}{(2n)!!}, \quad J_0 = 1$$

and

$$(2n)!! = 2.4.6.\ldots\ldots(2n)$$

$$(2n-1)!! = 1.3.5.\ldots\ldots(2n-1)$$

in Eq. (2.14), we obtain

$$L(\eta) = \frac{4C_0}{\tan\delta\sqrt{1-\eta^2}} + \frac{4\tan\delta}{\pi}\int_0^1 \sum_{n=1}^{\infty} \epsilon_{2n}\eta_i^{2n} \sum_{m=0}^{\infty} J_{2m}\, a^{2m}\eta_i^{2m}$$

$$\times \ln\left[\frac{\sqrt{1-\eta^2}+\sqrt{1-\eta_i^2}}{\sqrt{1-\eta^2}-\sqrt{1-\eta_i^2}}\right] d\eta_i$$

(2.16)

Let

$$I_{2k} = \int_0^1 \eta^{2k} \ln \frac{\sqrt{1-\eta^2} + \sqrt{1-\eta_i^2}}{\sqrt{1-\eta^2} - \sqrt{1-\eta_i^2}} \, d\eta_i .$$

Integrating by parts and simplifying we find

$$I_{2k} = \frac{2\sqrt{1-\eta^2}}{2k+1} \int_0^1 \frac{\eta_i^{2(k+1)}}{(\eta_i^2 - \eta^2)\sqrt{1-\eta^2}} \, d\eta_i$$

$$= \frac{\pi}{2k+1} (1-\eta^2)^{1/2} \sum_{i=0}^{k} J_{2i} \, \eta^{2(k-i)} . \qquad (2.17)$$

Hence (2.16) may now be expressed as

$$L(\eta) = \frac{4 C_0}{\tan\delta \sqrt{1-\eta^2}} + \frac{4 \tan\delta}{\pi} \sum_{n=1}^{\infty} \epsilon_{2n} \sum_{m=0}^{\infty} J_{2m} \, a^{2m} \, I_{2(m+n)} \qquad (2.18)$$

The constant C_0 in (2.12) which determines the strength of the leading edge singularity is given by

$$C_0 = -\frac{\tan^2\delta}{E(k)} \epsilon_0 + \frac{\tan^2\delta}{E(k)} \left[-\sum_{n=1}^{\infty} \frac{\epsilon_{2n}}{2n} - \frac{2a^2}{\pi} K(k) \right.$$

$$\times \sum_{n=1}^{\infty} \epsilon_{2n} \int_0^1 \eta^{2n} \sqrt{\frac{1-\eta^2}{1-a^2\eta^2}} \, d\eta + \frac{2}{\pi} K(k) \sum_{n=1}^{\infty} \epsilon_{2n} \int_0^1 \eta^{2n-1}$$

$$\left. \times \int_0^{\phi} (1 - a^2 \sin^2\phi)^{1/2} \, d\phi \, d\eta - \frac{2}{\pi} \left[K(k) - E(k) \right] \right.$$

$$\times \sum_{n=1}^{\infty} \epsilon_{2n} \int_0^1 \eta^{2n-1} \int_0^{\phi} (1-a^2 \sin^2\phi)^{-1/2}\, d\phi\, d\eta \Big] . \qquad (2.19)$$

In solving this we need to solve for certain integrals which are evaluated below.

$$R_{2n} = \int_0^1 \eta^{2n} \sqrt{\frac{1-\eta^2}{1-a^2\eta^2}}\, d\eta$$

On putting $\eta = \sin\theta$, we have

$$R_{2n} = \int_0^{\pi/2} \sin^{2n}\theta \cos^2\theta\, (1-a^2\sin^2\theta)^{-1/2}\, d\theta$$

$$= \frac{1}{2} B\left(\frac{2n+1}{2}, \frac{3}{2}\right) F\left(\frac{2n+1}{2}, \frac{1}{2}; \frac{2n+4}{2}; a^2\right) \qquad (2.20)$$

where B is the complete Beta function and F the hypergeometric function.

Similarly for the integral appearing in the third term inside the square brackets in (2.19) we have

$$\int_0^1 \eta^{2n-1} \int_0^{\phi} (1-a^2\sin^2\phi)^{1/2}\, d\phi\, d\eta$$

$$= \frac{1}{2n} \left[E(a) - S_{2n} \right] \qquad (2.21)$$

where

$$S_{2n} = \int_0^1 \eta^{2n} \sqrt{\frac{1-a^2\eta^2}{1-\eta^2}}\, d\eta$$

$$= \frac{1}{2} B\left(\frac{2n+1}{2}, \frac{1}{2}\right) F\left(\frac{2n+1}{2}, \frac{1}{2}; \frac{2n+2}{2}, a^2\right) \qquad (2.22)$$

and finally for the integral in the last term we find

$$\int_0^1 \eta^{2n-1} \int_0^{\phi} (1-a^2\sin^2\phi)^{-1/2}\, d\phi\, d\eta$$

$$= \frac{1}{2n}\left[K(a) - T_{2n}\right]$$

(2.23)

Where

$$T_{2n} = \int_0^1 \eta^{2n} \frac{d\eta}{\sqrt{1-a^2\eta^2}\sqrt{1-\eta^2}}$$

$$= \frac{1}{2} B\left(\frac{2n+1}{2}, \frac{1}{2}\right) F\left(\frac{2n+1}{2}, \frac{1}{2}; \frac{2n+2}{2}; a^2\right).$$

Hence (2.19) now becomes

$$C_0 = -\frac{\tan^2\delta}{E(k)}\epsilon_0 + \frac{\tan^2\delta}{E(k)}\left\{\left(\frac{2}{\pi}K(k)\left[E(a) - K(a)\right]\right.\right.$$

$$\left. + \frac{2}{\pi}E(k)K(a) - 1\right) \sum_{n=1}^{\infty} \frac{\epsilon_{2n}}{2n}$$

$$\left. - \sum_{n=1}^{\infty} \frac{\epsilon_{2n}}{n\pi}\left[\left(2n a^2 K_{2n} + S_{2n} - T_{2n}\right)K(k) + I_{2n}E(k)\right]\right\}.$$

(2.25)

Eqs. (2.18) and (2.25) together determine the pressure distribution at any chordwise station for a conically cambered delta wing with subsonic leading edges and a twist distribution given by (2.15).

The spanwise distribution of lift is given by

$$C_l(\eta) = \frac{1}{c_r C_L} \int_{x_1}^{1} L(\eta_i)\, dx$$

$$= \frac{\eta}{c_r C_L} \int_{\eta}^{1} L(\eta_i) \frac{d\eta_i}{\eta_i^2} . \qquad (2.26)$$

On substituting for $L(\eta_1)$ in (2.26) we have

$$C_l(\eta) = \frac{1}{c_r C_L} \left[\frac{4 C_0 \sqrt{1-\eta^2}}{\tan\delta} + \frac{4\tan\delta}{\pi} \eta \int_{\eta}^{1} \sum_{n=1}^{\infty} \epsilon_{2n} \right.$$

$$\left. \times \sum_{m=0}^{\infty} J_{2m} \frac{a^{2m}}{\eta_i^2} I_{2(m+n)}\, d\eta_i \right]$$

$$= \frac{1}{c_r C_L} \left[\frac{4 C_0 \sqrt{1-\eta^2}}{\tan\delta} + \frac{4\tan\delta}{\pi} \sum_{n=1}^{\infty} \epsilon_{2n} \right.$$

$$\left. \times \sum_{m=0}^{\infty} J_{2m}\, a^{2m}\, Q_{2(m+n)} \right] \qquad (2.27)$$

where

$$Q_{2k} = \eta \int_{\eta}^{1} \frac{I_{2k}}{\eta_i^2}\, d\eta_i$$

$$= \frac{\pi}{2k+1} \sum_{i=0}^{k} J_{2i}\, \eta \int_{\eta}^{1} (1-\eta^2)^{1/2}\, \eta_i^{2(k-i-1)}\, d\eta_i$$

$$= \frac{\pi}{2k(2k+1)} (1-\eta^2)^{3/2} \left[\eta^{2(k-1)} + \sum_{m=1}^{k-1} \frac{(2m+1)!!}{(2m)!!} \eta^{2(k-m-1)} \right. .$$

(2.28)

For the surface shape at any chordwise station, we start from

$$\frac{\partial z}{\partial x} = \frac{w(\eta)}{U} \tag{2.29}$$

and the z-coordinate distribution

$$z = x\bar{z}\ (y/x\tan\delta) = x\bar{z}(\eta) \tag{2.30}$$

so that

$$\frac{\partial z}{\partial x} = \bar{z}(\eta) - \eta\frac{\partial \bar{z}}{\partial \eta} = w(\eta) \tag{2.31}$$

and the spanwise surface slope is

$$\frac{\partial z}{\partial y} = \frac{1}{\tan\delta}\frac{\partial \bar{z}}{\partial \eta}\ . \tag{2.32}$$

Integrating (2.31) we obtain

$$\bar{z}(\eta) = K\eta - \eta\int \frac{w(\eta)}{\eta^2}\,d\eta \tag{2.33}$$

where K is an arbitrary constant and shows that the wing shapes are non-unique to the extent that a dihedral angle does not affect the aerodynamic characteristics in the linearized theory. In further analysis K is put equal to zero, i.e. no dihedral.

On solving (2.32) for the twist distribution (2.15) we have

$$\bar{z}(\eta) = -\sum_{k=1}^{\infty} \epsilon_{2k}\frac{\eta^{2k}}{2k\,(2k-1)} - \epsilon_0 \tag{2.34}$$

and

$$z(\eta) = x\bar{z}(\eta)$$

gives the ordinate of the wing at any point on the wing.

When the ordinate is measured with respect to the wing median surface, we have

$$Z = z(x,y) - z(x,0) = x\left[\bar{z}(\eta) - \bar{z}(0)\right]$$

$$= -x \sum_{k=1}^{\infty} \epsilon_{2k} \frac{\eta^{2k}}{2k(2k-1)} \quad . \tag{2.35}$$

The spanwise slope is then

$$\frac{\partial Z}{\partial \eta} = -x \sum_{k=1}^{\infty} \epsilon_{2k} \frac{\eta^{2k-1}}{2k-1} \quad . \tag{2.36}$$

The lift and drag coefficients are calculated using the surface values of the pressure and the downwash. The lift dependent drag coefficient is, therefore,

$$C_D = -\int_0^1 L(\eta)\, w(\eta)\, d\eta$$

$$= \int_0^1 \sum_{i=0}^{\infty} \epsilon_{2i}\, L_{2i}(\eta) \sum_{j=0}^{\infty} \epsilon_{2j}\, w_{2j}(\eta)\, d\eta \tag{2.37}$$

where L_{2i} is the pressure distribution due to the twist distribution $w_{2i} = \eta^{2i}/2i$.

Now define

$$l_i = \int_0^1 L_{2i}(\eta)\, d\eta$$

$$d_{ij} = -\int_0^1 L_{2i}(\eta)\, w_{2j}(\eta)\, d\eta \qquad (2.38)$$

then

$$C_D = \epsilon_0 \sum_{i=0}^{\infty} \epsilon_{2i}\, l_i + \sum_{i=0}^{\infty}\sum_{j=1}^{\infty} \epsilon_{2i}\, \epsilon_{2j}\, d_{ij}. \qquad (2.39)$$

The expression for l_1 is

$$l_i = \int_0^1 L_{2i}(\eta)\, d\eta, \qquad i > 0$$

$$= \frac{4\tan\delta}{\pi} \sum_{m=0}^{\infty} J_{2m}\, a^{2m} \int_0^1 I_{2(m+i)}\, d\eta$$

$$= \frac{4\tan\delta}{\pi} \sum_{m=0}^{\infty} J_{2m}\, a^{2m} \frac{\pi}{2(m+i)+1}$$

$$\times \sum_{j=0}^{m+i} J_{2j} \int_0^1 (1-\eta^2)^{1/2}\, \eta^{2(m+i-j)}\, d\eta$$

or

$$l_i = \frac{4\tan\delta}{\pi} \sum_{m=0}^{\infty} J_{2m}\, a^{2m} \frac{\pi}{2(m+i)+1}$$

$$\times \sum_{j=0}^{m+i} J_{2j}\, G_{2(m+i-j)} \qquad (2.40)$$

where

$$G_{2k} = \int_0^1 (1-\eta^2)^{1/2}\, \eta^{2k}\, d\eta = \frac{\pi}{2}\,\frac{(2k-1)!!}{(2k+2)!!}\,; \quad G_0 = \frac{\pi}{4}\,. \tag{2.41}$$

The expression for l_0 which corresponds to the flat plate case is

$$l_0 = \frac{4\tan\delta}{E(k)}\,. \tag{2.42}$$

The expression for d_{ij} is

$$d_{ij} = -\int_0^1 L_{2i}(\eta)\, w_{2j}(\eta)\, d\eta$$

$$= -\frac{4\tan\delta}{\pi} \sum_{m=0}^{\infty} J_{2m}\, a^{2m}\, \frac{\pi}{2(m+i)+1} \sum_{k=0}^{m+i} G_{2(m+i+j-k)}\, J_{2k}\,. \tag{2.43}$$

Notice that $l_i = -d_{i0}$.

The lift coefficient is given by

$$C_L = \int_0^1 L(\eta)\, d\eta$$

$$= \sum_{i=0}^{\infty} \epsilon_{2i}\, l_i \tag{2.44}$$

where l_i are given by (2.40) and (2.42).

The collection of results (2.18), (2.25), (2.27), (2.35),

(2.36), (2.39) and (2.44) give the necessary aerodynamic and geometric characteristics.

2.3 Discussion of Results

In section (2.2), the aerodynamic and geometric properties of a class of conically cambered delta wings with subsonic leading edges were presented. The geometrical properties are especially easy to visualise when the wing has a single twist distribution of the type $w_{2n} \sim \eta^{2n}/2n$. Thus, one may immediately see that for $n > 0$ the wing will have drooped leading edges and with increasing values of n, the central portion of the wing will become more and more flat. The droop becomes noticeable towards the outboard side and rapidly increases as it nears the leading edge. If one defines an arbitrary point η_0 as the location where $z(\eta_0) - z(0) = |\delta|$, and δ is some specified constant, then for a given δ, η_0 will move outboard rapidly with increasing n.

The spanwise surface slope will be low in the central portion of the wing but will rapidly increase as it progresses near the leading edge. A similar trend will be shown by the angle of attack distribution, which will be positive in the central portion and will move to negative values near the leading edge. There will be a continuous decrease in the angle of attack from the root to the tip, a property that alleviates tip stall. The droop near the leading edge will help the flow to turn smoothly, and hence may be expected to

predict properties closer to the real situation. The wings are also easy to manufacture and do not possess kinks.

The aerodynamic properties are a little more difficult to visualize. We restrict the following discussion to cases where the load vanishes at the leading edge. If reference is made to Tables 2.1 and 2.2 and Figures 2.2a-2.2d, it is noticed that the wing properties depend strongly on the amount of spanwise curvature for a given lift. Thus, with decreasing curvature (increasing n), the wing incidence decreases and moves towards the flat plate value, and the suction peak moves outboard and increases in magnitude. The spanwise load distribution tends towards the ideal elliptic distribution and progressively decreases the drag coefficient and the efficiency factor and increases the L/D ratio.

The spanwise load distribution, unlike the flat plate which shows infinite slope at the leading edge, has zero slope; the magnitude of the load distribution increases at the centre, and decreases outboard near the leading edge as compared to the plane delta wing with suction. The effect is progressively less pronounced with increasing n. This kind of behaviour is to be expected since the angle of attack decreases from the root to the tip and the wing tip is less loaded compared to a plane delta wing. This gives better tip stall characteristics.

The suction peak which increases in magnitude and moves outboard with increasing n, acts on the forward facing area of the drooped edge and thereby produces a thrust force which

TABLE 2.1 : OVERALL AERODYNAMIC CHARACTERISTICS OF BASIC SHAPES

Wing (n)	C_D	L/D	e	α_o	a
1	.00109	91.65	1.371	.032	0.10
2	.00098	101.52	1.238	.024	
3	.00094	106.46	1.180	.021	
4	.00091	109.4	1.149	.020	
Flat Plate (with Suction)	.00083	121.18	1.034	.016	
Flat Plate (w/o Suction)	.00162	61.70	2.038	.016	
1	.00151	66.31	1.805	.035	0.50
2	.00140	71.38	1.760	.027	
3	.00135	73.81	1.702	.025	
4	.00132	75.24	1.670	.023	
Flat Plate (with Suction)	.00124	80.76	1.555	.019	
Flat Plate (w/o Suction)	.00193	51.82	2.421	.019	
1	.00182	54.80	2.203	.037	0.70
2	.00172	58.07	2.164	.029	
3	.00168	59.57	2.109	.027	
4	.00165	60.44	2.079	.025	
Flat Plate (with Suction)	.00157	63.56	1.974	.021	
Flat Plate (w/o Suction)	.00214	46.70	2.602	.021	

e = efficiency factor = $AR\ C_D / C_L^2$ α_o = Wing incidence

$\tan\delta = 1.0$ $C_L = 0.10$

TABLE 2.2 : AERODYNAMIC AND GEOMETRIC CHARACTERISTICS OF BASIC WINGS

$a = 0.50$

Wing (n)	η	$\frac{L(\eta)}{C_L}$	$\ell(\eta)$	$\frac{\alpha(\eta)\tan\delta}{C_L}$	$\frac{z(\eta)\tan\delta}{x\,C_L}$	$\left(\frac{\partial z}{\partial \eta}\right)\frac{\tan\delta}{C_L}$
1	.00	.842	.842	.350	-.000	-.024
	0.20	.891	.794	.327	-.024	-.238
	0.40	1.018	.653	.256	-.095	-.475
	0.60	1.164	.438	.137	-.214	-.713
	0.70	1.203	.313	.059	-.291	-.832
	.80	1.174	.187	-.030	-.380	-.951
	0.90	.992	.072	-.131	-.481	-1.070
	0.95	.766	.027	-.186	-.536	-1.129
	1.00	.000	.000	-.239	-.589	-1.185
2	0.00	.760	.760	.273	-.000	-.000
	0.20	.788	.735	.272	-.000	-.006
	0.40	.891	.650	.258	-.005	-.050
	0.60	1.109	.487	.197	-.025	-.168
	0.70	1.248	.372	.133	-.047	-.267
	0.80	1.356	.239	.034	-.080	-.399
	0.90	1.296	.100	-.110	-.128	-.568
	0.95	1.068	.038	-.203	-.159	-.667
	1.00	0.000	.000	-.300	-.193	-.768

TABLE 2.2 (Contd.)

$a = 0.50$

wing (n)	η	$\frac{L(\eta)}{C_L}$	$\frac{c}{b}(\eta)$	$\frac{\alpha \tan\delta}{C_L}$	$\frac{z \tan\delta}{\alpha C_L}$	$\left(\frac{\partial z}{\partial \eta}\right)\frac{\tan\delta}{C_L}$
3	0.00	.725	.725	.247	-.000	-.000
	.20	.747	.705	.247	-.000	-.000
	0.40	.827	.638	.244	-.001	-.008
	0.60	1.035	.506	.218	-.006	-.057
	0.70	1.215	.405	.174	-.014	-.124
	0.80	1.425	.275	.085	-.032	-.242
	0.90	1.514	.122	-.081	-.065	-.437
	0.95	1.328	.049	-.206	-.091	-.572
	1.00	.000	.000	-.352	-.121	-.722
4	0.00	.706	.706	.233	-.000	-.000
	0.20	.725	.688	.233	-.000	-.000
	0.40	.794	.629	.233	-.000	-.001
	0.60	.976	.514	.222	-.002	-.021
	0.70	1.164	.423	.196	-.005	-.062
	0.80	1.435	.300	.123	-.016	-.157
	0.90	1.668	.142	-.049	-.040	-.358
	0.95	1.550	.058	-.201	-.062	-.523
	1.00	.000	.000	-.307	-.091	-.724

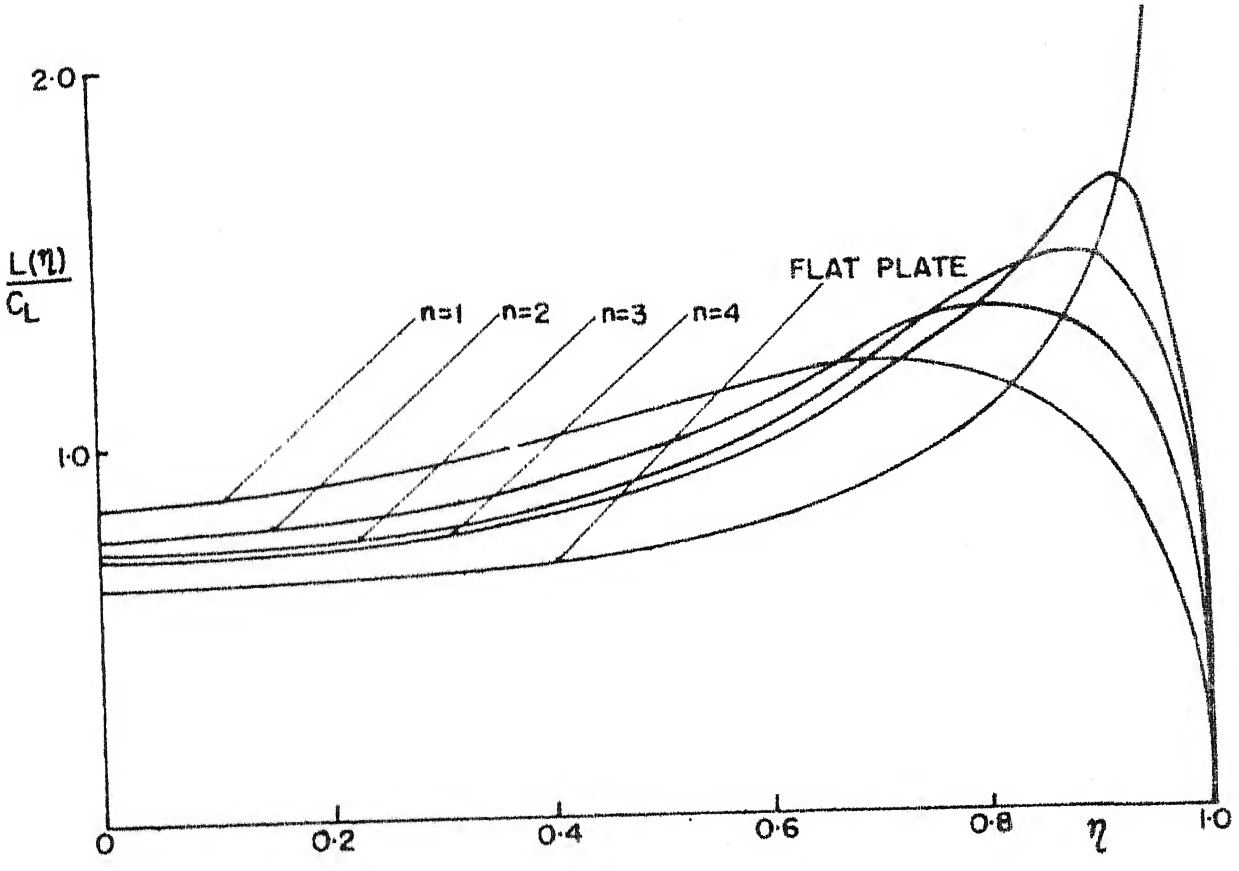

FIG. 2.2a. SPANWISE PRESSURE DISTRIBUTION (a=0·50)

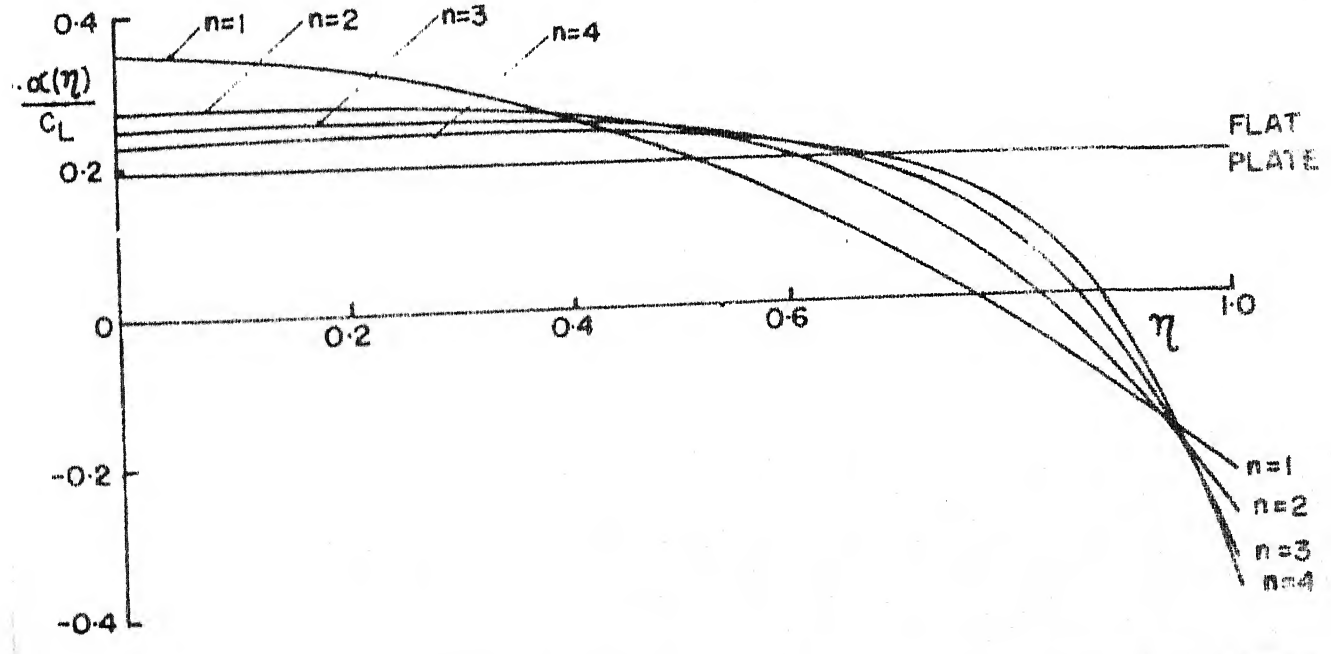

FIG. 2.2b. SPANWISE ANGLE OF ATTACK DISTRIBUTION (a=0·50)

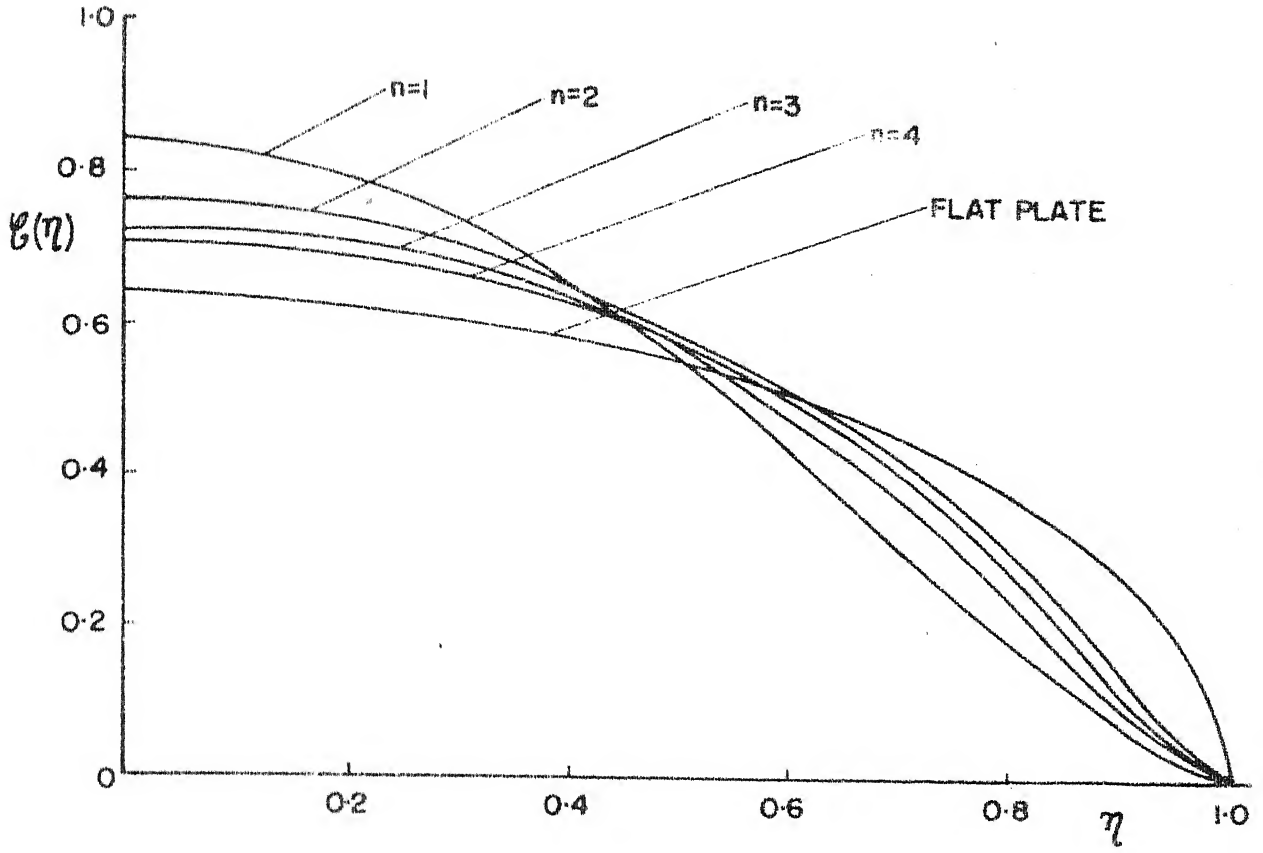

FIG.2.2c SPANWISE LIFT DISTRIBUTION (a=0·50)

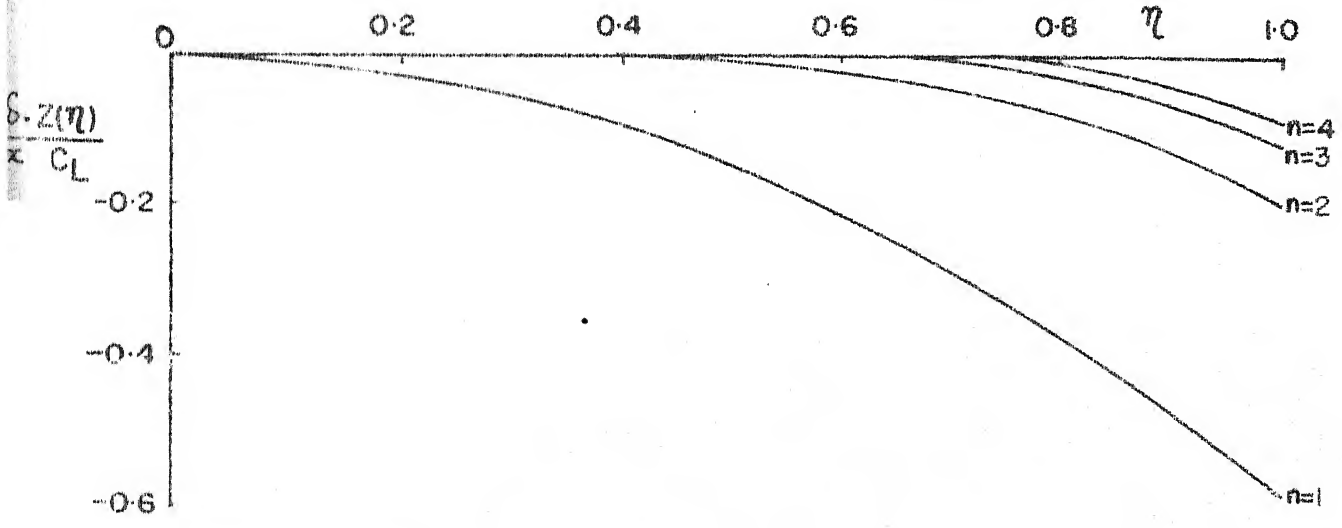

FIG.2.2d. SPANWISE ORDINATE DISTRIBUTION (a=0·50)

helps to reduce drag. For n=4, the C_D is substantially close to the flat plate value with suction. For a given n it approaches the flat plate drag faster with increasing values of a. The leading edge thrust obtainable in a plane delta wing due to leading edge suction, is obtained in the case of a cambered wing with a leading edge droop. Thus, the cambered wings, when compared with a flat delta neglecting leading edge thrust, are definitely superior aerodynamically.

Conically cambered wings may show some advantages over other shapes under off-design conditions. Thus, at any supersonic speed, the load will vanish at the leading edge at some incidence and, therefore, the attachment line is unlikely to lie on the upper surface for part of the wing and on the lower surface for the remainder, even away from the design incidence and Mach number.

Conical camber may be restrictive, since a control over the pitching moment is not possible. The chordwise distribution of load is linear and the aerodynamic centre is always at the centre of area. This may be remedied by using a parabolic camber or some of the results of Lance[11,12]. However, the simplicity of the surface shapes may be lost.

For wings lying near the axis of the Mach cone, the wave drag due to lift is a relatively small part of the lift-dependent drag and conical camber may be fruitfully used.

For wings with leading edges close to the Mach cone, when the wave drag due to lift exceeds the vortex drag, conical camber will not be very useful.

It is possible by choosing higher powers of η that one may come as close to the flat plate value as desired, however, the spanwise surface slopes and the magnitude of the tip incidence will become very large and the small perturbation assumptions are likely to be violated.

From a practical point of view it would be interesting to find upto what value of n the wings would be useful. Inviscid potential flow theory provides no answer. The matter, in practice, is closely connected to the design C_L, M and the various basic shapes that are combined to produce the wing since they determine the adverse pressure gradients which the boundary layer must overcome. They will also determine, to a certain extent, the state of the boundary layer.

From the analytical results mentioned in Section 2.2, the low aspect ratio results may be obtained by putting a=0. These results may then be used, as done by Weber, to design wings of arbitrary planforms and downwash distribution by takin the constants ϵ_{2n} as functions of the streamwise coordinate, x.

And finally, from Eq. (2.15) one notices that the pressure distribution will remain the same if the term $\frac{d\varphi}{d\eta} \cdot \frac{1}{\sqrt{1-a^2}}$

in the integral remains the same. We can, therefore, for a given pressure distribution, find the downwash distribution required at a given Mach number and apex angle. This is easy in our case since w is expressed in even powers of η and $1/\sqrt{1-a^2\eta^2}$ may be expanded in similar powers for $a < 1$, and the results of section 2.2 may be applied. An interesting feature is noticed from Table 2.3 that for a given value of n and C_L the spanwise pressure distribution and the spanwise lift distribution differ little for different values of a, although the wing shapes and twist distributions are quite different. Thus one would conclude that the wing root bending moment would be about the same for these cases.

TABLE 2.3 : COMPARISON OF WINGS AT DIFFERENT VALUES OF 'a' FOR THE BASIC SHAPES*

n = 2

η	$L(\eta)/C_L$			$\mathcal{C}(\eta)$		
	a=0.1	a=0.5	a=0.7	a=0.1	a=0.5	a=0.7
0.00	.764	.760	.757	.764	.760	.757
0.20	.791	.788	.783	.738	.735	.731
0.40	.897	.891	.884	.651	.650	.648
0.60	1.115	1.109	1.099	.485	.487	.489
0.70	1.251	1.248	1.242	.369	.372	.376
0.80	1.350	1.356	1.363	.236	.239	.243
0.90	1.276	1.296	1.324	.098	.100	.103
0.95	1.045	1.068	1.104	.037	.038	.040
1.00	.000	.000	.000	.000	.000	.000

η	$\alpha(\eta)\tan\delta/C_L$			$z\tan\delta/x\,C_L$		
	a=0.1	a=0.5	a=0.7	a=0.1	a=0.5	a=0.7
0.00	.241	.273	.293	-.000	-.000	-.000
0.20	.240	.272	.293	-.000	-.000	-.000
0.40	.225	.258	.280	-.005	-.005	-.004
0.60	.159	.197	.225	-.027	-.025	-.023
0.70	.089	.133	.167	-.051	-.047	-.042
0.80	-.019	.034	.078	-.087	-.080	-.072
0.90	-.175	.110	-.052	-.139	-.128	-.115
0.95	-.276	-.203	-.135	-.172	-.159	-.143
1.00	-.382	-.300	-.223	-.208	-.193	-.173

* Variations of quantities with a is slow, whereas results of Tsien, Holla, etc. show marked changes. Hence, off-design behaviour of our wings is expected to be much better particularly in terms of drag in a real flow.

TABLE 2.3 (Contd.)

n = 4

η	$L(\eta)/C_L$			$\mathcal{C}(\eta)$		
	$a=0.1$	$a=0.5$	$a=0.7$	$a=0.1$	$a=0.5$	$a=0.7$
0.00	.707	.706	.704	.707	.706	.704
0.20	.726	.725	.723	.689	.688	.686
0.40	.796	.794	.791	.630	.629	.628
0.60	.982	.978	.971	.514	.514	.515
0.70	1.169	1.164	1.156	.422	.423	.425
0.80	1.437	1.435	1.430	.298	.300	.303
0.90	1.657	1.668	1.685	.140	.142	.145
0.95	1.529	1.550	1.584	.057	.058	.060
1.00	.000	.000	.000	.000	.000	.000

η	$\alpha \tan\delta / C_L$			$z \tan\delta / x C_L$		
	$a=0.1$	$a=0.5$	$a=0.7$	$a=0.1$	$a=0.5$	$a=0.7$
0.00	.202	.233	.255	-.000	-.000	-.000
0.20	.202	.233	.255	-.000	-.000	-.000
0.40	.201	.233	.255	-.000	-.000	-.000
0.60	.189	.222	.245	-.002	-.002	-.001
0.70	.160	.196	.222	-.006	-.005	-.005
0.80	.080	.123	.158	-.017	-.016	-.014
0.90	-.110	-.049	.007	-.045	-.040	-.035
0.95	-.279	-.201	-.127	-.069	-.062	-.055
1.00	-.496	-.397	-.299	-.100	-.091	-.080

CHAPTER 3

OFF DESIGN PERFORMANCE

3.1 Off-Design Calculations ($\Delta\alpha$, ΔM)

The off-design performance of a wing must be satisfactory to make it acceptable for use. About the design incidence and Mach number, it is, therefore, desirable to know how much penalty one pays if the incidence or the Mach number or both change by small values. Of principal interest is the pressure distribution, the spanwise loading and the lift and drag coefficients since these present a comprehensive picture of the wing's aerodynamic efficiency. Linearised theory is assumed to be valid.

3.1.1 Increase in angle of attack, $\Delta\alpha$

The effect of an increment in incidence $\Delta\alpha$, can be obtained by superimposing the pressure distribution of a flat delta at an incidence $\Delta\alpha$. The flat plate results are known, and the off-design results are given below. Hence

$$L(\eta)_{off} = L(\eta)_{des} + \frac{4\tan\delta\ \Delta\alpha}{E(k)\sqrt{1-\eta^2}} \qquad (3.1)$$

$$C_l(\eta)\ c(\eta)_{off} = C_l(\eta)\ c(\eta)_{des} + \frac{4\tan\delta}{E(k)}\ \Delta\alpha\ \alpha(1-\eta^2)^{1/2} \qquad (3.2)$$

$$C_{L_{off}} = C_{L_{des}} + \frac{2\pi \tan\delta}{E(k)} \Delta\alpha \qquad (3.3)$$

and the drag coefficient is

$$C_{D_{off}} = \int_0^1 \left(L_{des} + \frac{4\tan\delta\ \Delta\alpha}{E(k)\sqrt{1-\eta^2}} \right) (\alpha_{des} + \Delta\alpha)\, d\eta$$

$$= C_{D_{des}} + C_{L_{des}} \Delta\alpha - \frac{2\pi \tan\delta}{E(k)} \Delta\alpha$$

$$\times \left[\sum_{n=1}^{\infty} \epsilon_{2n} \frac{(2n-1)!!}{2n\,(2n)!!} - \Delta\alpha - \epsilon_0 \right] \qquad (3.4)$$

where the subscript 'off' refers to off-design conditions and 'des' to the design condition.

3.1.2 Increase in Mach number, ΔM

A change in the Mach number implies a change in the slenderness parameter, a. Let us define

$$(a + \Delta a)^2 = \left[(M + \Delta M)^2 - 1 \right] \tan^2\delta. \qquad (3.5)$$

The expression for the pressure distribution is

$$L_{off} = \frac{4\,(C_0 + \Delta C_0)}{\tan\delta\sqrt{1-\eta^2}} + \frac{4\tan\delta}{\pi} \int_0^1 \frac{dw}{d\eta_i} \frac{\eta_i}{\sqrt{1-(a+\Delta a)^2\eta_i^2}}$$

$$\times \ln \left[\frac{\sqrt{1-\eta^2} + \sqrt{1-\eta_i^2}}{\sqrt{1-\eta^2} - \sqrt{1-\eta_i^2}} \right] d\eta_i . \qquad (3.6)$$

Expanding in a binomial series the term

$$\left[1-(a+\Delta a)^2\eta_i^2\right]^{-1/2} \simeq 1+\tfrac{1}{2}a^2\eta_i^2+a\Delta a\eta_i^2+\cdots \qquad (3.7)$$

where Δa is the change in a due to ΔM change in the Mach number and ΔC_0 is the corresponding change in C_0.

On substituting (3.7) into (3.6) and retaining terms containing upto Δa^2 we obtain

$$L_{off} = L_{des.} + \frac{4\Delta C_0}{\tan\delta\sqrt{1-\eta^2}} + \frac{4\tan\delta}{\pi}\int_0^1 \sum_{n=1}^{\infty} \epsilon_{2n}\,\eta_i^{2n+2}\,(a\Delta a+\tfrac{1}{2}\Delta a^2) \times \ln\left[\frac{\sqrt{1-\eta^2}+\sqrt{1-\eta_i^2}}{\sqrt{1-\eta^2}-\sqrt{1-\eta_i^2}}\right] d\eta_i$$

$$= L_{des} + \frac{4\Delta C_0}{\tan\delta\sqrt{1-\eta^2}} + \frac{4\tan\delta}{\pi}\sum_{n=1}^{\infty}\epsilon_{2n}\,(a\Delta a+\tfrac{1}{2}\Delta a^2)\,I_{2n+2} \qquad (3.8)$$

$$\mathcal{C}(\eta)_{off} = \mathcal{C}(\eta)_{des} + \frac{1}{C_2 C_1}\left[\frac{4\Delta C_0\sqrt{1-\eta^2}}{\tan\delta} + \frac{4\tan\delta}{\pi} \times \sum_{n=1}^{\infty}\epsilon_{2n}\,(a\Delta a+\tfrac{1}{2}\Delta a^2)\,Q_{2(n+1)}\right] \qquad (3.9)$$

and the lift coefficient may immediately be written down as

$$C_{L_{off}} = \int_0^1 L(\eta)_{off}\, d\eta$$

$$= C_{L_{des}} + \frac{2\pi \Delta C_0}{\tan\delta} + 4\tan\delta \sum_{n=1}^{\infty} \epsilon_{2n} \frac{(a\Delta a + \frac{1}{2}\Delta a^2)}{2n+3}$$

$$\times \sum_{k=0}^{n+1} J_{2k}\, G_{2(n+1-k)}. \qquad (3.10)$$

The expression for ΔC_0 is obtained as follows:

$$C_0 + \Delta C_0 = \frac{\tan^2\delta}{E(k)} \left[-\epsilon_0 - \sum_{n=1}^{\infty} \frac{\epsilon_{2n}}{2n} - \frac{2a'^2 K(k)}{\pi} \sum_{n=1}^{\infty} \epsilon_{2n} R_{2n} \right.$$

$$+ \frac{2}{\pi} K(k) \sum_{n=1}^{\infty} \epsilon_{2n} \left\{ E(a') - S_{2n} \right\} / 2n$$

$$\left. - \frac{2}{\pi} \left\{ K(k) - E(k) \right\} \sum_{n=1}^{\infty} \epsilon_{2n} \left\{ \frac{K(a') - T_{2n}}{2n} \right\} \right] \qquad (3.11)$$

where

$$a' = a + \Delta a$$

Now writing the elliptic integrals K and E and the functions R, S and T in powers of a and retaining the first few terms in Δa, we obtain after some algebra,

$$\Delta C_0 = -\Delta a^2 \frac{\pi}{8} \frac{\tan^2\delta}{E^2(a)} \left\{ -\frac{2a^2}{\pi} K(k) \sum_{n=1}^{\infty} \epsilon_{2n} B\left(\frac{2n+1}{2}, \frac{3}{2}\right) \right.$$

$$\times \left(a + 3a^2 \frac{2n+3}{n+3} \right) - \frac{a\Delta a}{2} \sum_{n=1}^{\infty} \epsilon_{2n} \left[R_{2n} + \frac{E(a) - S_{2n}}{2n} \right.$$

$$\left. \left. - \frac{1}{n} \left(K(a) - T_{2n} \right) \right] + \sum_{n=1}^{\infty} \epsilon_{2n} B\left(\frac{2n+1}{2}, \frac{1}{2}\right) \frac{2n+1}{n+1} \Delta a \right.$$

$$\left[\frac{4K(k)}{\pi} \left(a + \frac{2n+2}{n+2} 4a^3 \right) - \frac{2}{\pi} E(k) \left(a + \frac{2n+3}{n+2} 3a^2 \right) \right] \Bigg\} \qquad (3.12)$$

where the functions B, K and E are defined in Chapter 2. Notice that the change in C_o due to ΔM is of the order of $(\Delta a)^2$.

The drag coefficient is

$$C_{D_{off}} = \int_0^1 L_{off}\, \alpha_{des}\, d\eta = -\int_0^1 L_{off} \left(\epsilon_0 + \sum_{j=1}^{\infty} \epsilon_{2j} \frac{\eta^{2j}}{2j} \right) d\eta$$

$$= C_{D_{des}} - \frac{2\pi C_o}{\tan\delta} \left[\epsilon_0 + \sum_{n=1}^{\infty} \frac{\epsilon_{2n}}{2n(2n+1)} \right]$$

$$+ 4\tan\delta \sum_{n=1}^{\infty} \epsilon_{2n} \frac{\left(a\Delta a + \frac{1}{2}\Delta a^2 \right)}{2n+3}$$

$$\times \sum_{k=0}^{n+1} J_{2k} \left[\sum_{j=1}^{\infty} \epsilon_{2j}\, G_{2(n+j-k+1)} \frac{1}{2j} + \epsilon_0\, G_{2(n-k+1)} \right]. \qquad (3.13)$$

3.2 Off-Design at High Incidences

At high incidences, leading edge vortices appear which modify the pressure distribution over the wing considerably and there is evidence that for a delta wing with sharp leading edges, the vortex development is almost conical in nature. Here following Kuchemann[54] and Squire [55] we assume that the leading edge vortices modify the flow in such a way that the

additional average downwash is equal to the increase in incidence from the design condition of zero load at the leading edge. Additional assumptions are that for this case the load at the leading edge remains zero and the additional vortex lift is equal in magnitude to the leading edge force as predicted by the attached flow theory, acting perpendicular to the leading edge in the plane of the wing. This was shown to be substantially true for flat delta and delta type wings by Polhamus[56] and is assumed to be true here. Apart from these, the additional flow field due to the vortex system is supposed to adjust itself so that it presents least drag for itself. To solve the problem use is made of the conical solution obtained earlier in Chapter 2.

Hence the downwash condition is

$$\int_0^1 \alpha(\eta)\, d\eta = \Delta\alpha$$

or

$$\epsilon_0 + \sum_{n=1}^{\infty} \frac{\epsilon_{2n}}{2n\,(2n+1)} = -\Delta\alpha \qquad (3.14)$$

where $\Delta\alpha$, the increment in the angle of attack may be large.

The zero load condition is obtained by putting $C_0 = 0$ in Eq. (2.25)

$$\epsilon_0 - \sum_{n=1}^{\infty} \frac{\epsilon_{2n}}{2n} \left\{ \left(\frac{2}{\pi} K(k) \left[E(a) - K(a) \right] + \frac{2}{\pi} K(a)\, E(k) - 1 \right) \right.$$

$$-\frac{2}{\pi}\left[\left(\pi a^2 R_{2n} + S_{2n} - T_{2n}\right) K(k) + T_{2n} E(k)\right]\Bigg\} = 0$$

or

$$\epsilon_0 - \sum_{n=1}^{\infty} \epsilon_{2n} A_{2n} = 0 \tag{3.15}$$

where the definition of A_{2n} is obvious.

The suction analogy of Polhamus yields

$$\sum_{n=1}^{\infty} \epsilon_{2n} l_n = \frac{C_{Ds}}{\sin\delta} + C_{L_{att}} = C_{L_v} + C_{L_{att}}$$

$$= \frac{\pi \tan\delta\,(\Delta\alpha)^2}{E^2(k)} (1-a^2)^{1/2} \frac{1}{\sin\delta} + \frac{2\pi \tan\delta\,\Delta\alpha}{E(k)}$$

or

$$\sum_{n=1}^{\infty} \epsilon_{2n} l_n = \frac{\pi\Delta\alpha}{E(k)}\left[\frac{\sec\delta\sqrt{1-a^2}\,\Delta\alpha}{E(k)} + 2\tan\delta\right] \tag{3.16}$$

where C_{L_v} and $C_{L_{att}}$ are the lift coefficients due to the leading edge vortex and that due to the attached potential flow theory for $\Delta\alpha$, respectively.

The complete problem would now read, if a finite number (N) of conical solutions are used,

Minimize $$C_D = \sum_{i=1}^{N}\sum_{j=1}^{N} \epsilon_{2i}\,\epsilon_{2j}\,d_{ij} + \epsilon_0 \sum_{i=1}^{N} \epsilon_{2i}\,l_i \tag{3.17}$$

subject to

$$\epsilon_o + \sum_{n=1}^{N} \epsilon_{2n} / 2n(2n+1) = -\Delta\alpha \tag{3.18}$$

$$\epsilon_o - \sum_{n=1}^{N} \epsilon_{2n} A_{2n} = 0 \tag{3.19}$$

$$\sum_{n=1}^{\infty} \epsilon_{2n} l_n = \frac{\pi \Delta\alpha}{E(k)} \left[\frac{\sec\delta \sqrt{1-a^2}\ \Delta\alpha}{E(k)} + 2\tan\delta \right] \tag{3.20}$$

which may be solved for the unknown constants ϵ_{2n} using the Lagrange multiplier method. The additional pressure distribution ΔL due to the leading edge vortex may be obtained by introducing these constants in Eq. (2.18).

The total pressure distribution is

$$L(\eta)_{off} = L_{des} + \Delta L \tag{3.21}$$

and the total lift is

$$C_{L_{off}} = C_{L_{des}} + C_{L_{att}} + C_{L_v} \tag{3.22}$$

3.3 Discussion of Results

For small deviations in α and M, the wings show good characteristics as indicated by Table 3.1. From a design condition of a = 0.5, C_L = 0.10, and $\tan\delta$ = 1, a 20% change in the angle of attack did not substantially alter the L/D ratio or the efficiency factor compared to a wing designed for the off-design cases. Similarly for a 10% change in a,

TABLE 3.1 OFF DESIGN PERFORMANCE OF CONICALLY CAMBERED DELTA WINGS FOR n = 2 AND 4 (a=0.5, tanδ = 1.0)

	n = 2					n = 4				
	α_0	$\Delta\alpha = 0.2\alpha_0$		$\Delta\alpha = -0.2\alpha_0$		α_0	$\Delta\alpha = 0.2\alpha_0$		$\Delta\alpha = -0.2\alpha_0$	
		off-des.	des	off-des	des		off des	des	off-des	des
C_L	0.1000	0.1283	0.1200	0.0717	0.0800	0.1000	0.1242	0.1200	0.0758	0.0800
C_D	0.001400	0.002252	0.002252	0.000856	0.000720	0.001330	0.002041	0.002052	0.000845	0.000764
L/D	71.38	56.96	51.28	83.71	111.11	75.24	60.87	58.48	89.66	104.71
e	1.760	1.719	2.042	2.092	1.414	1.670	1.663	1.791	1.848	1.500
α_0	0.02728	0.03274	0.03274	0.02182	0.02182	0.02333	0.02800	0.02800	0.01866	0.01866

	a=0.5	$\Delta a = 0.1a$		$\Delta a = -0.1a$		a=0.5	$\Delta a = 0.1a$		$\Delta a = 0.1a$	
		off des	des	off-des	des.		off - des.	des.	off-des.	des
C_L	0.1000	0.1105	0.981	0.0905	0.1018	0.1000	0.1195	0.1151	0.0824	0.1196
C_D	0.001400	0.001687	0.001426	0.001140	0.001387	0.001330	0.001785	0.001864	0.000918	0.001799
L/D	71.38	65.51	68.79	79.36	73.40	75.24	66.95	61.75	89.68	66.48
e	1.760	1.736	1.861	1.749	1.682	1.670	1.571	1.768	1.699	1.579
α_0	0.02728	.02728	.02728	0.02728	0.02333	0.02333	0.02333	0.02333	0.02333	0.02333

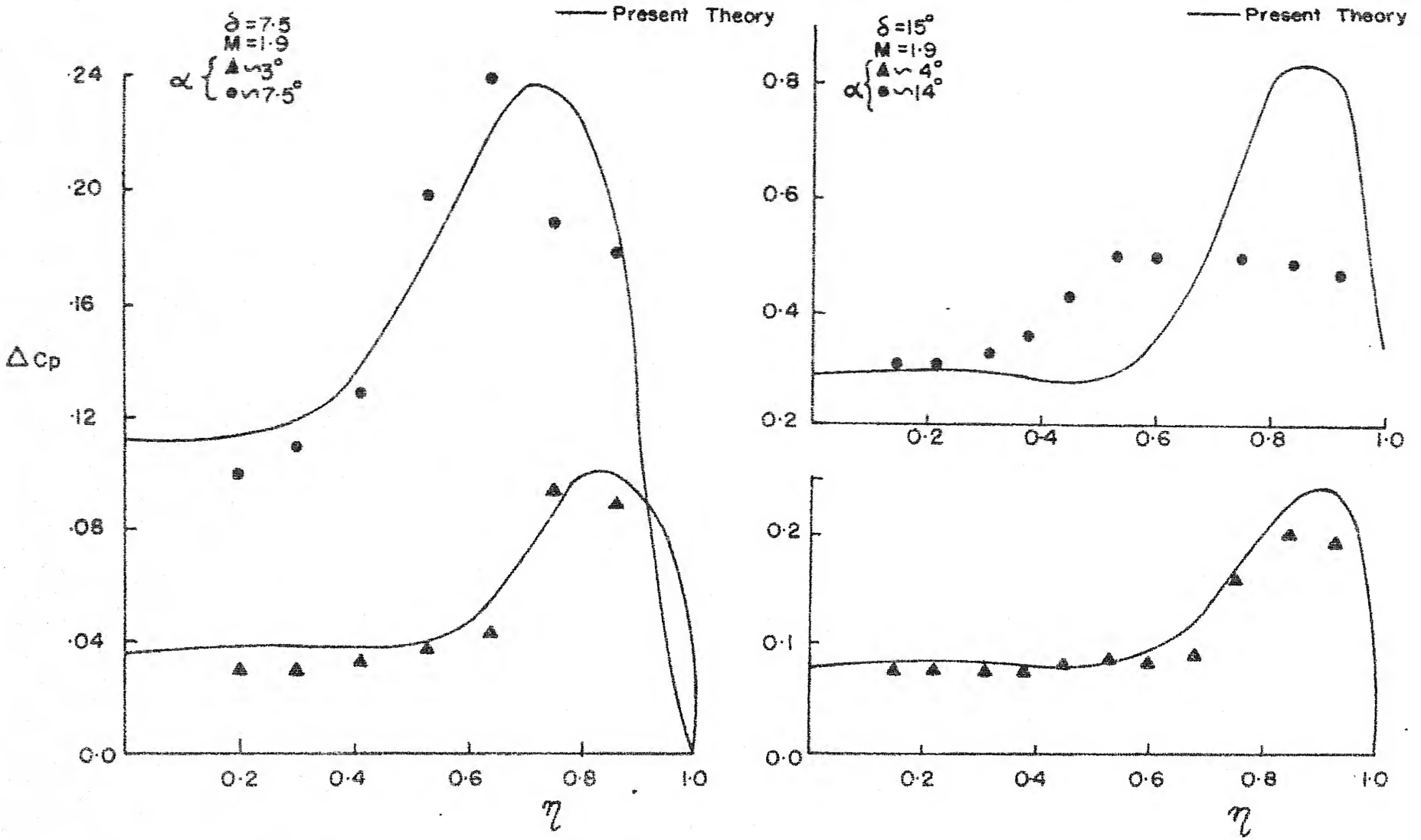

FIG. 3.1. SPANWISE PRESSURE DISTRIBUTION AT HIGH INCIDENCES

—— Plane Delta

the same trend was noticed. The wings may, therefore, be considered for practical use.

For large deviations in α where leading edge vortices are observed*, experimental results are available only for a plane delta[18] hence theoretical results are compared with these. A reference to Figure 3.1 shows good agreement, in general, with the experimental pressure distributions for low aspect ratios. The comparison for the case $\delta = 15^{\circ}$, $\alpha = 14$ shows marked deviations. This is the largest incidence shown and indicates that at such high incidence, the non-linear thickness effect is probably very important, a fact neglected in our analysis. It is also possible that secondary vortices have developed and have influenced the pressure distribution. This fact is also not accounted for in the analysis.

---

* Large deviations are used in the sense that leading edge vortices have developed and have a significant effect.

CHAPTER 4

SOME THEORIMS CONCERNING DRAG MINIMIZATION

4.1 Introduction

One of the central problems in aerodynamics has been the finding of minimum drag configurations for wings, bodies and their combinations. The literature in the past fifty years has evolved theorems that generally identify a minimum drag configuration, but seldom say how to arrive at it. In deriving the minimum drag theorems the combined flow field concept and the reverse flow theorems have been widely used. The combined flow field, first introduced by Munt, is defined as the flow field obtained by superimposing the disturbance velocities in forward and reverse flow over a body having a given distribution of lift, sideforce, and thickness. The reverse flow theorem for wings can be stated in a compact way as[37-39]

$$\int p_F \alpha_R \, dA = \int p_R \alpha_F \, dA \tag{4.1}$$

where p and α are respectively the pressure and angle of attack distribution, and F and R refer to the forward and reverse flows. The integration is over the wing surface. The theorem is valid for subsonic, supersonic, steady and unsteady flow situations.

In the following section we derive some theorems which are essentially generalizations of those given by Rodriguez, et. al.[33] The interesting feature of these theorems is that they help us in deciding how to proceed in order to reduce drag. The results derived are valid only if there is no leading edge suction, e.g. the conical wings of this dissertation. The following definitions hold:

$$d_{ij} = \int p_i \alpha_j \, dA \quad \text{and} \quad l_i = \int p_i \, dA .$$

4.2 The Theorems

Theorem 1. Any combination of two loadings (p_1, α_1) and (p_2, α_2) supporting a given total lift will have less drag than either loading supporting the same total lift provided

$$2 d_{11} / (d_{12} + d_{21}) < l_1 / l_2 . \tag{4.2}$$

Proof: Let (p_1, α_1) and (p_2, α_2) be two non-orthogonal loadings. Then after Graham, a pair of orthogonal loadings is given by

$$\left.\begin{aligned} \underset{\sim}{p}_1 &\equiv (\underset{\sim}{p}_1, \underset{\sim}{\alpha}_1) = (p_1, \alpha_1) \\ \underset{\sim}{p}_2 &\equiv (\underset{\sim}{p}_2, \underset{\sim}{\alpha}_2) = (p_1 + c p_2, \; \alpha_1 + c \alpha_2) \end{aligned}\right\} \tag{4.3}$$

where

$$c = - 2 d_{11} / (d_{12} + d_{21}) . \tag{4.4}$$

Since $\underset{\sim}{p}_1$ and $\underset{\sim}{p}_2$ are orthogonal loadings, they may be combined in any manner to reduce drag, provided each is supporting a positive life, i.e.

$$\int \underset{\sim}{p}_1 \, dA > 0 \qquad \text{and} \qquad \int \underset{\sim}{p}_2 \, dA > 0 . \tag{4.5}$$

Hence it follows that

$$-2d_{11} / (d_{12} + d_{21}) = c > -\int p_1 \, dA / \int p_2 \, dA = l_1 / l_2 \tag{4.6}$$

which is what we wanted to prove.

It must be noted that the condition postulated by this theorem can always be satisfied by a proper choice of signs for the loadings. It thus determines which of the loadings, if any, should carry a negative lift. The theorem, however, does not say anything about their magnitudes and may be chosen arbitrarily to the extent that it satisfies the lift constrain

Theorem 2. If (p_1, α_1) and (p_2, α_2) are two loadings in forward flow satisfying the condition $2d_{11} / (d_{12} + d_{21}) < l_1 / l_2$, then the corresponding loadings $(\tilde{p}_1 = p_1, \ \tilde{\alpha}_1)$ and $(\tilde{p}_2 = p_2, \ \tilde{\alpha}_2)$ in reverse flow will also satisfy a similar condition.

Proof: Since $\tilde{p}_1 = p_1$ and $\tilde{p}_2 = p_2$, hence $\tilde{l}_1 = l_1$ and $\tilde{l}_2 = l_2$ where the curly bar on top denotes quantities in reverse flow.

Also

$$d_{12} = \int p_1 \alpha_2 \, dA = \int \tilde{p}_1 \alpha_2 \, dA = \int p_2 \tilde{\alpha}_1 \, dA = \int \tilde{p}_2 \tilde{\alpha}_1 \, dA = \tilde{d}_{21}$$

Similarly $d_{21} = \tilde{d}_{12}$.

Hence the condition:

$$2 d_{11} / (d_{12} + d_{21}) < l_1 / l_2$$

also reads

$$2 \tilde{d}_{11} / (\tilde{d}_{12} + \tilde{d}_{21}) < \tilde{l}_1 / \tilde{l}_2$$

which proves the theorem.

The importance of this theorem is that it is sometimes easier to deal with a wing in reverse flow than in forward flow and the above theorem lets us choose the easier way.

Theorem 3. If a loading (p, α) is representable by a linear combination of loadings (p_i, α_i); $i = 1, 2, \ldots, N$ such that $p = \sum_{i=1}^{N} \epsilon_i p_i$ and $\alpha = \sum_{i=1}^{N} \epsilon_i \alpha_i$ then the constants ϵ_i are determined from the set of equations $\sum_{i=1}^{N} \epsilon_i (d_{ik} + d_{ki}) = \int (p \alpha_k + p_k \alpha) \, dA, \quad k = 1, 2, \ldots,$

Proof: Substituting the expansions for p and α in the right hand side of the above expression gives the result.

The importance of this result is that it allows us to determine the ϵ_i using an integral approach which is to be

preferred against a collocation procedure where the choice of the collocation points affect the ϵ_i . The result is presented in the same spirit as the evaluation of Fourier constants in a Fourier analysis.

Theorem 4. If the corresponding loadings in reverse flow are

$(\tilde{p}_i = p_i\,,\ \tilde{\alpha}_i)$ and

$\tilde{p} = \sum_{i=1}^{N} \tilde{\epsilon}_i \tilde{p}_i$ and $\tilde{\alpha} = \sum_{i=1}^{N} \tilde{\epsilon}_i \tilde{\alpha}_i$

then $\tilde{\epsilon}_i = \epsilon_i$

Proof: Since $\tilde{p}_i = p_i$, hence $a_{ik} + a_{ki} = \tilde{a}_{ik} + \tilde{a}_{ki}$ and from theorem 3 we have

$$\sum_{i=1}^{N} \tilde{\epsilon}_i \,(a_{ik} + a_{ki}) = \int (p\tilde{\alpha}_k + p_k \tilde{\alpha})\, dA$$

$$= \int (\tilde{p}\alpha_k + \tilde{p}_k \alpha)\, dA$$

$$= \int (p\alpha_k + p_k \alpha)\, dA$$

$$= \sum_{i=1}^{N} \epsilon_i \,(a_{ik} + a_{ki})\,.$$

Comparing both sides gives the desired result.

As a consequence of theorems 3 and 4 one may easily prove that if $(p_{opt}\,,\ \alpha_{opt})$ is an optimal loading in forward flow, then $(\tilde{p} = p_{opt}\,,\ \tilde{\alpha})$ is also optimal in reverse flow and

its expansion in terms of $(\tilde{\beta}_k, \tilde{\alpha}_k)$ has the same coefficients as in the corresponding forward flow.

4.3 Final Remarks

The importance of the above results lie in the fact, that given an arbitrary set of loadings, it is possible to move towards the minimum drag condition with considerable freedom, and thereby gives the designer considerable leeway in obtaining near optimal wing shapes which may be of greater use than the exact optimal in a real flow. Further, within the linearized theory, he has the option of working in either the forward or the reverse flow depending on the particular problem in hand.

CHAPTER 5

PRACTICAL METHODS OF DRAG MINIMIZATION-I.

5.1 Introduction

In the study of optimized wings, the problem of obtaining minimum drag wings subjected to a given total lift seems to have caught the widest attention. This problem has generally been solved by the Lagrange multiplier method. Grahm's orthogonal loading method[32], which is simpler, has found limited application presumably because the method of obtaining orthogonal loadings as outlined by him is cumbersome and unsuitable for digital computation. The theorems of Munk[29] and Jones[30, 31] for constructing minimum drag wings have also found little application except for an attempt by Ginzel and Multhopp[35].

In this chapter the Lagrange multiplier method is outlines because of its wide use and also for the sake of completeness. We follow this by giving a matrix representation of Grahm's orthogonal loading method and thus make it more suitable for digital computer applications. The matrix representation had eluded Graham[32] and his coworkers[33] since they mention that further research is necessary to get a better way of obtaining orthogonal loadings[33].

5.2 Lagrange Multiplier Method

The classical Lagrange multiplier (LM) method converts a constrained minimization problem to an unconstrained one. The prototype of this problem with equality constraints is

$$\text{Minimize} \quad f(\underset{\sim}{x}) \tag{5.1}$$

subject to

$$g_i(\underset{\sim}{x}) = b_i \quad , \quad i = 1, 2, \cdots, m \tag{5.2}$$

where the objective function $f(\underset{\sim}{x})$ and the constraint functions $g_i(\underset{\sim}{x})$ are functions of the n-vector $\underset{\sim}{x}$. The multiplier method requires one to form a new function

$$F(\underset{\sim}{x}, \underset{\sim}{\lambda}) = f(\underset{\sim}{x}) + \sum_{i=1}^{m} \lambda_i \left[g_i(\underset{\sim}{x}) - b_i \right] \tag{5.3}$$

and to solve the following simultaneous equations

$$\left.\begin{aligned} \frac{\partial f(\underset{\sim}{x}_0)}{\partial x_i} + \sum_{j=1}^{m} \lambda_j \frac{\partial g_j(\underset{\sim}{x}_0)}{\partial x_i} &= 0 , \qquad i = 1, 2, \cdots, n \\ g_j(\underset{\sim}{x}_0) &= b_j , \qquad j = 1, 2, \cdots, m \end{aligned}\right\} \tag{5.4}$$

where $\underset{\sim}{x} = \underset{\sim}{x}_0$ is the point at which $f(\underset{\sim}{x})$ takes on a relative minimum.

The drag minimization problem subject to a given lift may be stated as:

$$\text{Minimize} \quad C_D \equiv \sum_i \sum_j \epsilon_i \epsilon_j d_{ij} + \epsilon_0 \sum_i \epsilon_i l_i \tag{5.5}$$

subject to $$\sum_i \epsilon_i l_i = C_L . \tag{5.6}$$

The corresponding Lagrange function is

$$F = C_D + \lambda \left(\sum_i \epsilon_i l_i - C_L \right) \tag{5.7}$$

where the ϵ_i and λ for minimum drag are to be found from

$$\begin{aligned} \sum_j \epsilon_j (d_{ij} + d_{ji}) + \lambda l_i &= 0 \\ \sum_j \epsilon_j l_j &= C_L \end{aligned} \tag{5.8}$$

It may also be shown that at the minimum drag point

$$\lambda = -2 C_D / C_L \tag{5.9}$$

i.e. the Lagrange multiplier is twice the negative value of the optimum drag to lift ratio.

From physical considerations we know C_D is a strictly positive quantity. Further, if all the constraints in the problem are linear, it may be shown under certain conditions, to have a unique solution. The Lagrange multiplier method is useful in linearized wing theory because the drag is a quadratic function and the constraints to which the wing is subjected are often stated in a linear form. Thus the resulting equations corresponding to (5.4) are linear and may easily be solved by any of the standard methods for simultaneous linear equations.

5.3 Method of Orthogonal Loadings

Graham showed that the drag in the case of orthogonal

loadings was superposable. It was further shown by Graham that if one obtains a set of lifting pressure loadings, a linear combination of these, each carrying positive lift, would give smaller drag for a given total lift than any single member carrying the same total lift. (The corresponding result for non-orthogonal loadings is given by Theorem 1 of Chapter 4). It may also be shown that the absolute minimum in drag may be approached as close as desired by adding additional lifting loadings to the set.

5.3.1 Graham's method of orthogonalization

Given a set of loadings (p_k, α_k), $k=1,2,\ldots,m$, Graham proceeded to orthogonalize them as follows:

Let $P_i = (p_i, \alpha_i)$ be a pressure loading. Two pressure loadings are of different types if

$$p_i \neq \epsilon p_j \tag{5.10}$$

where ϵ is a constant, called the intensity of loading. Now suppose $P = (P_1, P_2, \ldots, P_m)$ is a set of non-orthogonal loadings and let $\underset{\sim}{P} = (\underset{\sim}{P}_1, \underset{\sim}{P}_2, \ldots, \underset{\sim}{P}_m)$, to be determined, be an orthogonal set derived from P. To start the process, Graham chose the first member $\underset{\sim}{P}$ as

$$\underset{\sim}{p}_1 = p_1 \; ; \qquad \underset{\sim}{\alpha}_1 = \alpha_1 . \tag{5.11}$$

The second member $\underset{\sim}{P}_2$ was chosen in the form

$$\underset{\sim}{p}_2 = p_1 + c p_2 \; ; \qquad \underset{\sim}{\alpha}_2 = \alpha_1 + c\alpha_2 \tag{5.12}$$

where from the orthogonality criterion

$$\int (\underset{\sim}{P}_2 \underset{\sim}{\alpha}_1 + \underset{\sim}{P}_1 \underset{\sim}{\alpha}_2)\, dA = 0 \tag{5.13}$$

we have

$$c = -2 d_{11} / (d_{12} + d_{21}). \tag{5.14}$$

Similarly the third member $\underset{\sim}{P}_3$ is obtained in the form

$$\underset{\sim}{P}_3 = \underset{\sim}{P}_1 + c_2 \underset{\sim}{P}_2 + c_3 \underset{\sim}{P}_3 \; ; \quad \underset{\sim}{\alpha}_3 = \alpha_1 + c_2 \alpha_2 + c_3 \alpha_3 \tag{5.15}$$

and again from the orthogonality criterion we have

$$\left.\begin{aligned} \int (\underset{\sim}{P}_3 \underset{\sim}{\alpha}_1 + \underset{\sim}{P}_1 \underset{\sim}{\alpha}_3)\, dA &= 0 \\ \int (\underset{\sim}{P}_2 \underset{\sim}{\alpha}_3 + \underset{\sim}{P}_3 \underset{\sim}{\alpha}_2)\, dA &= 0 \end{aligned}\right\} \tag{5.16}$$

or

$$\left.\begin{aligned} 2 d_{11} + c_2 (d_{12} + d_{21}) + c_3 (d_{13} + d_{31}) &= 0 \\ (d_{12} + d_{21}) + 2 c_2 d_{22} + c_3 (d_{23} + d_{32}) &= 0 \end{aligned}\right\} \tag{5.17}$$

from which c_2 and c_3 may be found.

Clearly; the process becomes laborious for successive members in the set and is not suitable for digital computers. Further, the orthogonal set is non-unique since the process could have been started with any member from the non-orthogonal set instead of the first one or with any linear combinations of them.

5.3.2 Orthogonal loadings - a matrix representation

5.3.2 Orthogonal loadings - a matrix representation

The drag expression may be written as

$$C_D = E \mathcal{A} E^T \tag{5.18}$$

where $E = \{ \epsilon_1, \epsilon_2, \ldots, \epsilon_n \}$ is a row vector in load intensities, and $\mathcal{A}$ is a symmetric matrix with elements

$$a_{ij} = \frac{1}{2} \int (p_i \alpha_j + p_j \alpha_i) \, dA. \tag{5.19}$$

The transformation to orthogonal loading requires diagonalization of the matrix $\mathcal{A}$. If $\mathcal{A}$ is non-singular and real, this is possible. Let G be a square matrix such that $G \mathcal{A} G^T$ results in a diagonal form. Hence

$$C_D = E G^{-1} G \mathcal{A} G^T G^{-T} E^T = \underset{\sim}{E} \underset{\sim}{\mathcal{A}} \underset{\sim}{E}^T \tag{5.20}$$

where

$$\underset{\sim}{\mathcal{A}} = G \mathcal{A} G^T \tag{5.21}$$

and

$$\underset{\sim}{E} = E G^{-1} \tag{5.22}$$

are respectively the diagonal matrix, and the intensity vector in the transformed space.

From matrix theory we know that G is not a unique transformation. One may use this non-uniqueness to choose G to suit certain computational requirements in diagonalising $\mathcal{A}$. We mention two methods of obtaining G. In the first

method, the eigenvalues of $\mathcal{A}$ are obtained and the corresponding eigenvectors are placed column by column to constitute . The diagonal matrix $\underset{\sim}{\mathcal{A}}$ then contains the eigenvalues in the diagonal. This method is well known and the matrix G in this case is known as the orthonormal modal matrix of $\mathcal{A}$. One may also remark that $\underset{\sim}{\mathcal{A}}$ may be reduced to a unit matrix by the transformation

$$\underset{\sim}{\epsilon_i} = \underset{\sim}{\epsilon_i} / \sqrt{\underset{\sim}{d_{ii}}} \tag{5.23}$$

The second method is to look for a matrix G which is triangular, i.e.

$$g_{ij} = 0 \quad \forall \quad j < i \tag{5.24}$$

and the non-zero elements are calculated from

$$\left.\begin{aligned} g_{ii}^2 &= A_i / A_{i-1} \\ g_{jk} &= \left(d_{jk} - \sum_{i=1}^{j-1} g_{ij}\, g_{ik}\right) / g_{jj}, \quad k = j+1, \ldots, n \end{aligned}\right\} \tag{5.25}$$

where A_i is determinant of the $(i \times i)$ principal minor of $\mathcal{A}$. Since the drag is a positive definite function, none of the A_n are zero. The second method implies that the first column vector of G is assumed coincident with the first loading, the second column vector is chosen to lie in the plane determined by the first and second loading, the third column vector is confined within the subspace determined by the first, second and third loadings, and so on. One realises that this is what the original Graham's method was trying to do.

5.3.3 A two constraint minimization problem

It may now be expected that the drag minimization calculation would be simplified. Consider, for example, the problem of obtaining minimum drag subject to a given lift and pitching moment constraint. The problem is

Minimize $C_D \equiv \sum_i \epsilon_i^2 d_{ii}$

subject to

$$\left.\begin{aligned} \sum_i \epsilon_i l_i &= C_L \\ \sum_i \epsilon_i m_i &= C_m \end{aligned}\right\} \qquad (5.26)$$

where d_{ii}, l_i, m_i are the drag, lift and pitching moment coefficients respectively due to unit intensity of the $i^{\underline{th}}$ member in the orthogonal set. C_L and C_m are the prescribed lift and pitching moment coefficients respectively. The corresponding unconstrained problem is

$$\text{Minimize } \sum_i \epsilon_i^2 d_{ii} + \lambda_1 \left(\sum_i \epsilon_i l_i - C_L \right) + \lambda_2 \left(\sum_i \epsilon_i m_i - C_m \right). \qquad (5.27)$$

The necessary conditions (5.4) show that

$$2 \epsilon_i d_{ii} + \lambda_1 l_i + \lambda_2 m_i = 0, \quad i = 1, 2, \ldots, n \qquad (5.28)$$

$$\left.\begin{aligned} \sum_i \epsilon_i l_i &= C_L \\ \sum_i \epsilon_i m_i &= C_m \end{aligned}\right\}. \qquad (5.29)$$

From (5.28) and (5.29) one may obtain

$$2 C_D + \lambda_1 C_L + \lambda_2 C_m = 0$$

or

$$\lambda_1 = -(\lambda_2 C_m + 2 C_D)/C_L \tag{5.30}$$

Substituting for λ_1 in (5.28) we obtain

$$\epsilon_i = \frac{1}{2 d_{ii}} \left[\frac{2 C_D l_i}{C_L} - \lambda_2 \left(m_i - \frac{C_m l_i}{C_L} \right) \right] \tag{5.31}$$

and substituting for ϵ_i in (5.29) we obtain

$$C_D = \frac{C_m^2 \sum_j \frac{l_j^2}{d_{jj}} - 2 C_m C_L \sum_j \frac{l_j m_j}{d_{jj}} + C_L^2 \sum_j \frac{m_j^2}{d_{jj}}}{\sum_j \frac{l_j^2}{d_{jj}} \sum_j \frac{m_j^2}{d_{jj}} - \left(\sum \frac{l_j m_j}{d_{jj}} \right)^2} \tag{5.32}$$

and solving for λ_2 gives

$$\lambda_2 = \frac{2 C_m - \frac{2 C_D}{C_L} \sum \frac{l_j m_j}{d_{jj}}}{\frac{C_m}{C_L} \sum \frac{l_j m_j}{d_{jj}} - \sum \frac{m_j^2}{d_{jj}}} \tag{5.33}$$

Equations (5.31) to (5.33) give the minimum value of the drag and the required load intensities ϵ_i. Setting $\lambda_2 = 0$ gives the results obtained in reference 32 for the case when only the lift constraint is present.

As a final remark, the Lagrange multiplier method when applied to non-orthogonal loadings may give rise to an ill-conditioned matrix and higher precision may be required to

to obtain reasonable results. The orthogonal loading method alleviates this problem and should be more suitable for numerical claculations. An additional advantage here is that one may always choose a proper sign for b_i so that l_i is positive, hence the intensities ϵ_i according to Graham must all be non-negative for the minimum drag problem subject to a given lift. This is a useful feature in mathematical programming formulations as will be shown in the next chapter.

CHAPTER 6

PRACTICAL METHODS OF DRAG MINIMIZATION-II.

6.1 Introduction

We continue in this chapter, the study of drag minimization techniques, and explore the possibility of using mathematical programming (MP) in order to introduce inequality constraints in addition to the equality constraints commonly used.* Mathematical programming has found wide applications in the optimization of structures, but very little in the aerodynamics of wings and bodies. By using MP one may introduce such constraints in the design problem as, for example, a suitable twist distribution near the wing tip for favourable tip stall, etc.

The general MP problem is

Minimize $f(\underset{\sim}{x})$

subject to

$$\begin{aligned} g_i(\underset{\sim}{x}) &\leq b_i \qquad i = 1, 2, \ldots, u \\ g_i(\underset{\sim}{x}) &\geq b_i \qquad i = u+1, \ldots, v \\ g_i(\underset{\sim}{x}) &= b_i \qquad i = v+1, \ldots, m \end{aligned} \tag{6.1}$$

and $x_j \geq 0 \qquad j = 1, 2, \ldots, n.$

---

*A reviewer has brought to the author's notice, after submission of this dissertation, that MP has been used to solve some thickness problems in wing-body aerodynamics in a paper by Haze, et.a J. Astronautical Sci., pp.283-296, 1968. We have used MP to solve lifting wing problems.

A particular feature of this formulation is that the unknown variables x_j are required to be non-negative. This allows one to obtain algorithms that work more efficiently by restricting the search to one orthant. However, any variable with unrestricted sign may be put in this form by defining two new non-negative variables x_j', x_j'', so that

$$x_j = x_j' - x_j''$$
$$x_j', x_j'' \geq 0 . \tag{6.2}$$

A problem in which $f(\underline{x})$ and all the $g_i(\underline{x})$ are linear is called a linear programming (LP) problem. A problem in which at least one of these functions is non-linear or has special restrictions placed on it (e.g. some or all x_j may be required to be integers) is called a non-linear programming (NLP) problem. A special case when $f(\underline{x})$ is a quadratic function and all the $g_i(\underline{x})$ are linear is called a quadratic programming(QP) problem. The drag minimization problem subject to linear constraints falls under the QP formulation. However, approximate LP formulations are also possible.

6.2 Linear Programming Method

The problem under consideration is restricted to the conical wing problem and for wings in subsonic flow. This problem allows control over the induced drag which is a minimum if the spanwise distribution of lift is elliptic. The formulation, therefore, requires a set of loadings to adjust their

intensities such that it satisfies the constraints in the problem, and follows the ideal elliptic spanwise distribution as closely as possible.

As an example, the problem of minimum drag subject to a given total lift is

$$\text{Minimize} \quad \delta \tag{6.3}$$

such that

$$\left.\begin{aligned} E(\eta_i) - \sum_j \epsilon_j C_j(\eta) &\leq \delta \\ -E(\eta_i) + \sum_j \epsilon_j C_j(\eta) &\leq \delta \end{aligned}\right\} \tag{6.4}$$

$$\sum_j \epsilon_j l_j = C_L \tag{6.5}$$

$$\epsilon_j \geq 0 \tag{6.6}$$

where (6.4) signify, in a discretized form, the constraint

$$\left| E(\eta) - \sum_j \epsilon_j C_j(\eta) \right| \leq \delta \tag{6.7}$$

and η_i are m-spanwise collocation points. $E(\eta)$ is the elliptic load distribution and $C_j(\eta)$ is the spanwise load distribution for the j^{th} loading of unit intensity. For the best fit obviously δ must be minimized. Also notice that $\epsilon_j \geq 0$. This will be so if the chosen loadings form an orthogonal set with each loading carrying positive lift. For other cases one may either orthogonalize the set or use (6.2).

The solution to the problem will give the intensities

and the maximum deviation δ between the ideal elliptic distribution and the actual distribution. The smaller the value of δ, smaller will be the drag which may be calculated once the ϵ_j are known. In the next chapter it will be shown that this method is good.

Additional equality and inequality constraints are easy to incorporate into the problem. These constraints may be used, for example, to restrict the solution to regions where the theoretical assumptions are valid. One might also require, for instance, the angle of attack not exceed a certain value, α_{Cait}, i.e.

$$\left| \sum_i \epsilon_i \alpha_i \right| \leq \alpha_{Cait} \tag{6.8}$$

This may be treated as two inequality constraints

$$\left.\begin{aligned} \sum_i \epsilon_i \alpha_i &\leq \alpha_{Cait} \\ -\sum_i \epsilon_i \alpha_i &\leq \alpha_{Cait} \end{aligned}\right\} \tag{6.9}$$

One might further introduce the constraint that $\alpha(\eta)$ should progressively decrease as one moves from the wing root to the tip, which in a discretized form would be

$$\sum_i \epsilon_i \alpha_i(\eta_j) - \sum_i \epsilon_i \alpha_i(\eta_{j+1}) \geq 0; \qquad j = 1, 2, \ldots, m-1 \tag{6.10}$$

where $|\eta_{j+1}| > |\eta_j|$. Such a twist distribution should alleviate problems of tip stall.

Various other constraints arising due to manufacturing requirements may be constructed and added to the constraints list in the problem. Thus the method immediately opens up a wider possibility of obtaining realistic wing shapes.

Several methods exist for solving LP problems. The output of which indicates whether the solution is feasible or not, if yes, whether it is bounded or not. If the solution is feasible and bounded, it gives the values of ϵ_j and δ.

6.3 Quadratic Programming Method

The drag being a quadratic function of the intensities ϵ_i, and within the framework of the linearized theory, many practical constraints can be expressed linearly in terms of ϵ_i. In this form the problem is

Minimize $$C_D = \sum_i \sum_j \epsilon_i \epsilon_j \alpha_{ij} \qquad (6.11)$$

subject to

$$\sum_i \epsilon_i l_i = C_L \qquad (6.12)$$

and other linear equality and inequality constraints some of which may be (6.9) and (6.10).

If one uses orthogonal loadings with each member carrying a positive lift, the problem may be written as

Minimize $$C_D = \sum_i \epsilon_i^2 \alpha_{ii} \qquad (6.13)$$

subject to

$$\sum_i \epsilon_i l_i = C_L \tag{6.14}$$

$$\sum_i \epsilon_i g_{ij} \left\{ \leq, =, \geq \right\} b_j, \quad j = 1, 2, \ldots, m \tag{6.15}$$

where (6.15) expresses the additional linear constraints on the problem, if any. The non-negativity condition on ϵ_i by virtue of orthogonality provided each $l_i > 0$ is automatically satisfied.

Several methods for solving QP problems exist in which the objective function is the sum of a linear and a quadratic function of the unknown variables. Prominent among these are the methods of Beale, and Wolfe which may be used.

6.4 Remarks

The Langrange multiplier method has been widely used in drag minimization problems. In comparison, the application of programming methods is of recent origin. It was shown, in this context, how LP and QP formulations may be usefully employed in drag minimization problems under inequality constraints and how orthogonal loadings may be useful in reducing the complexity of the problem. Use of orthogonal loadings also gives substantial benefits in computer core requirements.

Whereas the QP formulations are straightforward, the LP

formulations require one to choose a suitable objective function so that the resulting problem implies a drag minimization problem. The elliptic spanwise distribution of lift for minimum induced drag has been used in this chapter. However, on similar lines other drag minimization theorems may also be used, e.g. the combined flow field results of Munk and Jones.[1] This also provides a convenient vehicle for determining how sensitive minimum drag shapes are to small excursions from the theoretical minimum.

CHAPTER 7

COMPARISON OF DRAG MINIMIZATION METHODS AND OPTIMAL CONICAL WINGS

7.1 Introduction

A few examples are chosen to illustrate the drag minimization methods outlined in chapters 5 and 6. Also studied in this chapter are the wing shapes carrying a given total lift using various combinations of the first four basic twist distributions in the conical series of chapter 2 to provide design information. All examples are for $a = 0.5$ and $\tan\delta = 1.0$.

7.2 Comparative Study through Examples

Example 1. Minimize the drag subject to a given $C_L = 0.1$, using the first three basic conical twist distributions, i.e.

Minimize $$C_D = \sum_{i=1}^{3}\sum_{j=1}^{3} \epsilon_{2i}\,\epsilon_{2j}\,d_{ij} + \epsilon_0 \sum_{j=1}^{3} \epsilon_{2j}\,l_j$$

subject to

$$\sum_{i=1}^{3} \epsilon_{2i}\,l_i = 0.1$$

where ϵ_0 is related to the ϵ_{2i} through Equation (2.25) with $C_0 = 0$. The quantities d_{ij}, and l_i are calculated from Equations (2.40)-(2.43).

After substituting all the numbers we have,

Minimize $C_D = -0.141465\,\epsilon_2^2 - 0.120774\,\epsilon_4\,\epsilon_2 - 0.072186\,\epsilon_2\,\epsilon_6 - 0.024330\,\epsilon_4^2 - 0.028332\,\epsilon_4\,\epsilon_6 - 0.008131\,\epsilon_6^2 + 0.1\,\epsilon_0$

subject to

$$0.841243\,\epsilon_2 + 0.428166\,\epsilon_4 + 0.270535\,\epsilon_6 = 0.1$$

We have already noted in chapter 6 that mathematical programming methods require an additional constraint that all the unknown variables be non-negative. If this condition cannot be guaranteed apriori, an equivalent problem may be described using Equation (6.2) to define a set of new non-negative variables. An alternative method is to convert the given set of loadings to an orthogonal set using any of the methods given in chapter 5. Here we choose the diagonalization method using the eigenvalue technique. The above problem is now rewritten as

Minimize $C_D = 0.14168\,\epsilon_2'^2 + 0.63596\times10^{-3}\,\epsilon_4'^2 + 0.35390\times10^{-5}\,\epsilon_6'^2$

subject to $0.98171\,\epsilon_2' + 0.21284\times10^{-1}\,\epsilon_4' + 0.86737\times10^{-3}\,\epsilon_6' = 0.1.$

The matrix G of Equation (5.20) that accomplishes this is

$$G = \begin{bmatrix} 0.867299 & -0.483617 & 0.117936 \\ 0.423886 & 0.593294 & -0.684373 \\ 0.260988 & 0.643521 & 0.719561 \end{bmatrix}$$

and $\epsilon' = \epsilon G^{-1}$.

The solution to this problem is

$$\epsilon_2' = 0.0897, \qquad \epsilon_4' = 0.4331, \qquad \epsilon_6' = 3.1712$$

and

$$C_D = 0.001294.$$

This was solved using QP and the LM methods and was used to check out our QP computer program.

However, to solve the above problem using the LP method requires a linear objective function to replace the quadratic drag function. For this we follow the method outlined in chapter 6. Thus we write

Minimize δ

subject to

$$0.98171\,\epsilon_2' + 0.21284\times10^{-1}\,\epsilon_4' + 0.86737\times10^{-3}\,\epsilon_6' = 0.1$$

$$C_2'(\eta_j)\,\epsilon_2' + C_4'(\eta_j)\,\epsilon_4' + C_6'(\eta_j)\,\epsilon_6' - E(\eta_j) \le \delta$$

$$-C_2'(\eta_j)\,\epsilon_2' - C_4'(\eta_j)\,\epsilon_4' - C_6'(\eta_j)\,\epsilon_6' + E(\eta_j) \le \delta$$

$$\text{for } j = 1, 2, \ldots, n$$

and

$$\epsilon_2', \ \epsilon_4', \ \epsilon_6' \ge 0.$$

Here δ is a positive quantity to be minimized, $E(\eta)$ is the elliptic spanwise loading - a condition for minimum drag, $C_{2i}'(\eta)$ are the spanwise loadings due to the i^{th} orthogonal loading of unit intensity and $\eta = \eta_j$ are the collocation

points where the condition (6.7) is to be satisfied.

Several values of n were chosen. A sample of the results is given below:

1) $n = 3$; $\eta_j = 0.0, 0.3, 0.8$

$\epsilon_2' = 0.0890$, $\epsilon_4' = 0.5132$, $\epsilon_6' = 1.9781$, $\delta = 0.000246$

$C_D = 0.001304$

2) $n = 6$; $\eta_j = 0.0, 0.1, 0.3, 0.4, 0.8, 0.9$

$\epsilon_2' = 0.0874$, $\epsilon_4' = 0.4800$, $\epsilon_6' = 4.5451$, $\delta = 0.004223$

$C_D = 0.001302$

3) $n = 10$; $\eta_j = 0.0$ to 0.9 in steps of 0.1

$\epsilon_2' = 0.0877$, $\epsilon_4' = 0.4697$, $\epsilon_6' = 4.4582$, $\delta = 0.004534$

$C_D = 0.001300$.

Comparing the results with those of the QP (or LM) method we find that with increasing n , the C_D approaches the correct minimum. It may, therefore, be concluded that the LP method is a useful technique.

7.3 Minimum Drag Wings with Inequality Constraints

Minimum drag shapes under inequality constraints are of great practical significance. A few examples are given to illustrate the QP method.

Example 1. Using the basic twist distributions 1 and 3 minimize the drag subject to a given $C_L = 0.1$, a root incidence

between 0.03 and 0.04 radian, and a continuous washout in incidence from the wing root to the tip.

After orthogonalising the basic loads 1 and 3 and discretizing the washout constraint, the problem may be stated:

Minimize $C_D = 0.11627\ \epsilon_2'^2 + 0.36443 \times 10^{-3}\ \epsilon_6'^2$

subject to

$$0.88350\ \epsilon_2' + 0.17661 \times 10^{-1}\ \epsilon_6' = 0.1$$

$$\alpha_{i+1} - \alpha_i \leq 0, \qquad i = 0, 1, 2, \ldots, 11$$

$$\alpha_0 \leq 0.04$$

$$\epsilon_2', \epsilon_6' \geq 0$$

where

$$\alpha_i = \alpha(\eta_i)$$

$$\eta_0 = 0.0$$

$$\eta_{i+1} = \eta_i + 0.1, \qquad i = 1, 2, \ldots, 8$$

$$\eta_{10} = 0.95$$

$$\eta_{11} = 1.0$$

The results are

$$\epsilon_2' = 0.11010, \qquad \epsilon_6' = 0.15443, \qquad C_D = 0.001418$$

In comparison a wing designed only for $C_L = 0.1$ would have $C_D = 0.001321$. Thus the additional constraints in the example

have increased the drag coefficient by about $5\frac{1}{2}$ percent. In a real viscous medium this wing is likely to be better than the one designed with only the lift constraint which gives a wavy shape and a washout only near the tip. The wing shape and incidence distribution are shown in Fig.7.1 and compared against the case with only the lift constraint.

This example shows that it is possible with only two basic conical shapes to design a wing which satisfies a designer's notion of the desirable properties of a good wing in a viscous medium even by using an inviscid analysis, if one introduces inequality constraints. If one had solved the classical problem of drag minimization with only the lift constraint, this practically useful wing would not have been indicated.

Example 2. Using the basic twist distributions 2, 3 and 4 minimize the drag for a given $C_L = 0.1$, wing root incidence $\alpha_o = 0.03$ radian, $\partial z/\partial \eta \leq 0$ from wing root to tip and $\partial \alpha/\partial \eta \leq 0$ for $0.8 \leq |\eta| \leq 1.0$ and $z \geq -0.04$ at $\eta = 1.0$.

Orthogonalizing the basic loads and discretizing the probelm we have the following:

Minimize $C_D \equiv 0.40364 \times 10^{-1} \epsilon_4'^2 + 0.81546 \times 10^{-4} \epsilon_6'^2 +$

$+ 0.28572 \times 10^{-6} \epsilon_8'^2$

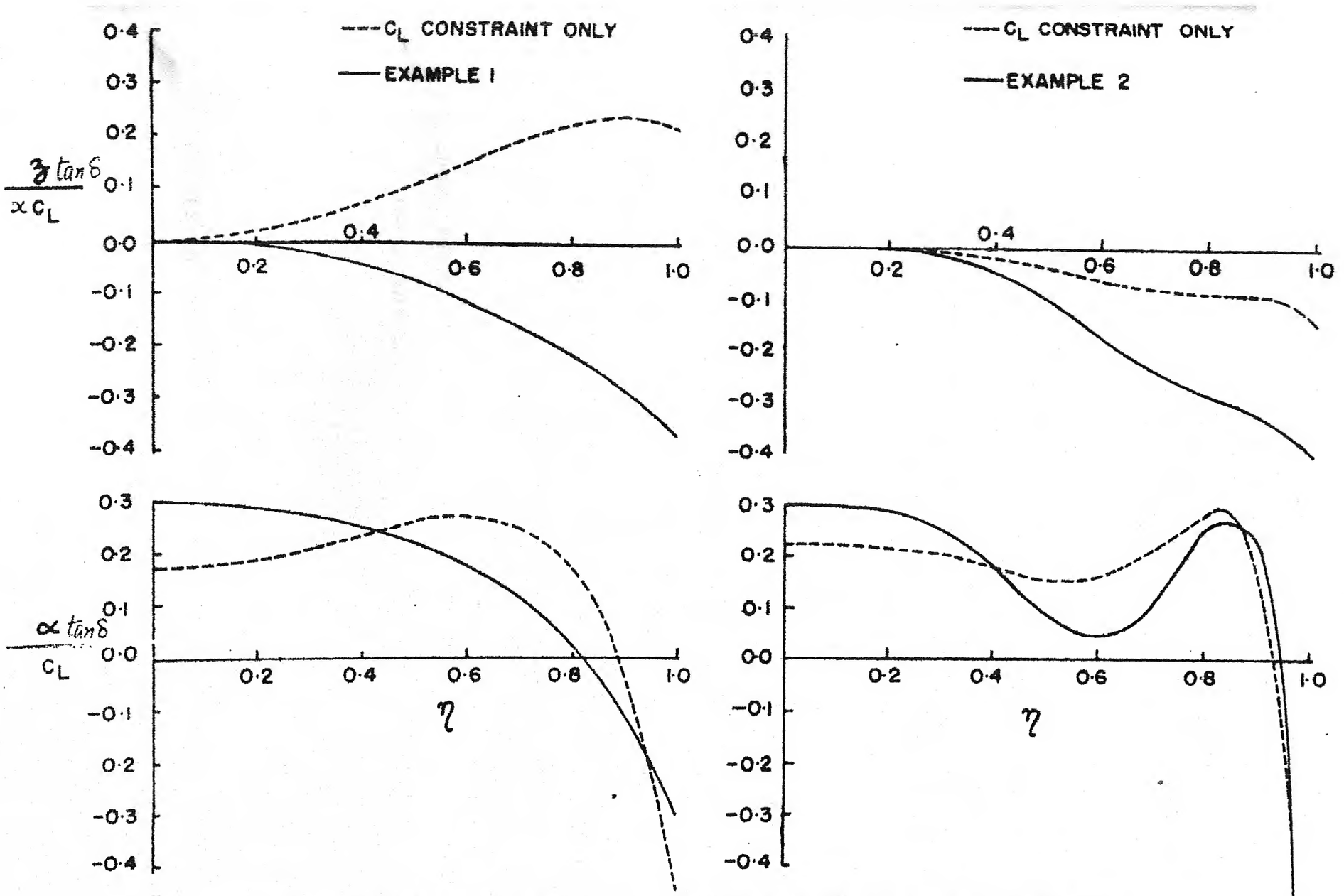

FIG.7.1. WING SHAPES AND INCIDENCE DISTRIBUTIONS OF EXAMPLES OF 1.&2.

subject to

$$Z_{i+1} - Z_i \leq 0, \qquad i = 0, 1, \ldots, 10$$

$$\alpha_{i+1} - \alpha_i \leq 0, \qquad i = 8, 9, 10$$

$$\alpha_0 = 0.03$$

$$Z_{11} \geq -0.04$$

$$\epsilon_4', \epsilon_6', \epsilon_8' \geq 0$$

where

$$\alpha_i = \alpha(\eta_i); \qquad Z_i = Z(\eta_i)$$

and the η_i are the same as in Example 1 above.

The results are

$$\epsilon_4' = 0.17389, \qquad \epsilon_6' = 0.40491, \qquad \epsilon_8' = 17.05696$$

$$C_D = 0.001317$$

But with only the lift constraint, $C_D = 0.001277$.

As for the previous example, the results are shown in Fig. 7.1. In this example the wing is restricted to have negative spanwise surface slope, and for favourable tip stall characteristics, a washout is prescribed in the outboard portion. The last constraint $Z_{11} \geq -0.04$ in the example means that a minimum clearance from a datum for the tip is specified.

This example again shows that our basic shapes are capable of configuring wing shapes to practical requirements with few members. Such problems for lifting wings do not

appear to have been solved earlier in the available literature. Nevertheless, these are the problems that are faced by wing designers, and MP methods have the potentiality of providing the necessary solutions.

Incidentally in the above examples, the LP method could also have been used as indicated in chapter 6 instead of the more accurate QP method used here.

7.4 Minimum Drag Wings for Given Lift

We close this chapter by studying the classical problem of minimum drag shapes obtainable by superimposing two or more of the first four basic distributions of chapter 2 in all possible combinations for a given total lift. Many of these shapes appear to be of practical use. The results are summarized in Tables (7.1) and (7.2). The wing shapes are drawn in Fig. 7.2.

Very systematic trends are observed as combinations of two, three and four of the basic twist distributions are used. For an even number of combinations it is noticed that the wing ordinates lie above the reference η-axis and for odd number of combinations they lie below.* Combinations of higher order

---

* Combinations of greater than four basic shapes were also calculated but are not shown in Tables (7.1) and (7.2). However, the comments made in this section reflect these results also.

TABLE 7.1 : AERODYNAMIC AND GEOMETRIC PROPERTIES OF OPTIMAL CONICAL WINGS (a = 0.5)

$L(\eta) / C_L$

Wings* η	12	13	14	23	24	34
0.0000	0.6381	0.6389	0.6395	0.6395	0.6396	0.6396
0.1000	0.6359	0.6388	0.6404	0.6413	0.6419	0.6422
0.2000	0.6344	0.6405	0.6442	0.6462	0.6483	0.6503
0.3000	0.6492	0.6516	0.6558	0.6535	0.6583	0.6628
0.4000	0.7032	0.6870	0.6850	0.6706	0.6753	0.6796
0.5000	0.8224	0.7718	0.7508	0.7216	0.7152	0.7084
0.6000	1.0268	0.9400	0.8874	0.8544	0.8189	0.7835
0.7000	1.3148	1.2234	1.1450	1.1335	1.0622	0.9916
0.8000	1.6276	1.6098	1.5613	1.5929	1.5300	1.4683
0.9000	1.7485	1.8991	1.9969	2.0485	2.1203	2.1924
0.9500	1.5186	1.7417	1.9312	1.9625	2.1349	2.3065
0.9950	0.5760	0.6956	0.8135	0.8139	0.9302	1.0464
1.0000	0.0000	0.0000	0.0000	0.0000	0.0000	0.0000

*Wing $i_1, i_2, \ldots i_k$ stands for wing designed to have a twist distribution, $\omega(\eta) = \epsilon_0 + \epsilon_{2i_1}\eta^{2i_1} + \epsilon_{2i_2}\eta^{2i_2} + \ldots + \epsilon_{2i_k}\eta^{2i_k}$;

e.g. Wing 12 has $\omega(\eta) = \epsilon_0 + \epsilon_2\eta^2 + \epsilon_4\eta^4$.

TABLE 7.1 (Contd.)

$L(\eta) / C_L$

Wings η	123	124	134	234	1234	Flat Plate
0.0000	0.6829	0.6785	0.6749	0.6710	0.6460	0.6368
0.1000	0.6918	0.6864	0.6816	0.6761	0.6458	0.6398
0.2000	0.7108	0.7051	0.7001	0.6939	0.6570	0.6497
0.3000	0.7190	0.7195	0.7215	0.7239	0.6995	0.6674
0.4000	0.7015	0.7144	0.7305	0.7523	0.7692	0.6946
0.5000	0.6735	0.6924	0.7162	0.7526	0.8189	0.7351
0.6000	0.7046	0.7024	0.7050	0.7227	0.7957	0.7958
0.7000	0.9237	0.8693	0.8156	0.7688	0.7655	0.8914
0.8000	1.4642	1.3797	1.2888	1.1864	1.0774	1.0610
0.9000	2.2030	2.2343	2.2560	2.2546	2.2205	1.4605
0.9500	2.2663	2.4164	2.5616	2.6880	2.8085	2.0388
0.9950	0.9938	1.1135	1.2311	1.3461	1.4761	6.3741
1.0000	0.0000	0.0000	0.0000	0.0000	0.0000	∞

TABLE 7.1 (Contd.)

$z \tan\delta / x\, C_L$

Wings η	12	13	14	23	24	34
0.0000	0.0004	0.0002	0.0001	0.0000	0.0000	0.0000
0.1000	0.0088	0.0044	0.0029	0.0000	0.0000	0.0000
0.2000	0.0346	0.0175	0.0115	0.0007	0.0004	0.0000
0.3000	0.0758	0.0393	0.0260	0.0035	0.0019	0.0003
0.4000	0.1293	0.0692	0.0461	0.0105	0.0059	0.0014
0.5000	0.1911	0.1062	0.0716	0.0231	0.0139	0.0049
0.6000	0.2560	0.1478	0.1016	0.0419	0.0271	0.0126
0.7000	0.3175	0.1895	0.1334	0.0644	0.0447	0.0255
0.8000	0.3682	0.2244	0.1614	0.0838	0.0619	0.0406
0.9000	0.3993	0.2412	0.1739	0.0868	0.0657	0.0452
0.9500	0.4044	0.2381	0.1682	0.0758	0.0548	0.0346
0.9950	0.4016	0.2261	0.1521	0.0547	0.0323	0.0107
1.0000	0.3984	0.2241	0.1496	0.0516	0.0289	0.0069

TABLE 7.1 (Contd.)

$2 \tan \delta / \pi C_L$

Wings	123	124	134	234	1234	Flat Plate
0.0000	-0.0005	-0.0004	-0.0002	-0.0000	-0.0005	0.0000
0.1000	-0.0120	-0.0087	-0.0050	-0.0001	-0.0119	0.0000
0.2000	-0.0462	-0.0338	-0.0200	-0.0015	0.0443	0.0000
0.3000	-0.0975	-0.0723	-0.0446	-0.0068	0.0883	0.0000
0.4000	-0.1581	-0.1197	-0.0770	-0.0185	0.1335	0.0000
0.5000	-0.2198	-0.1696	-0.1139	-0.0365	0.1721	0.0000
0.6000	-0.2753	-0.2157	-0.1497	-0.0567	0.2035	0.0000
0.7000	-0.3216	-0.2537	-0.1786	-0.0722	0.2348	0.0000
0.8000	-0.3632	-0.2852	-0.1992	-0.0780	0.2753	0.0000
0.9000	-0.4162	-0.3244	-0.2238	-0.0838	0.3205	0.0000
0.9500	-0.4563	-0.3573	-0.2490	-0.0988	0.3323	0.0000
0.9950	-0.5062	-0.4023	-0.2885	-0.1306	0.3232	0.0000
1.0000	-0.5129	-0.4086	-0.2943	-0.1429	0.3204	0.0000

TABLE 7.1 (Contd.)

$\alpha \tan\delta / C_L$

Wings η	12	13	14	23	24	34
0.0000	0.1568	0.1698	0.1764	0.1824	0.1855	0.1885
0.1000	0.1655	0.1742	0.1793	0.1825	0.1856	0.1885
0.2000	0.1899	0.1873	0.1879	0.1845	0.1866	0.1886
0.3000	0.2247	0.2085	0.2023	0.1924	0.1911	0.1898
0.4000	0.2612	0.2355	0.2219	0.2102	0.2027	0.1951
0.5000	0.2873	0.2626	0.2447	0.2385	0.2241	0.2099
0.6000	0.2871	0.2776	0.2639	0.2685	0.2529	0.2377
0.7000	0.2416	0.2586	0.2617	0.2756	0.2719	0.2685
0.8000	0.1280	0.1697	0.1978	0.2110	0.2323	0.2536
0.9000	-0.0798	-0.0440	-0.0089	-0.0087	0.0260	0.0604
0.9500	-0.2282	-0.2215	-0.2089	-0.2149	-0.1996	-0.1845
0.9550	-0.3915	-0.4349	-0.4730	-0.4779	-0.5133	-0.5484
1.0000	-0.4210	-0.4622	-0.5084	-0.5124	-0.5562	-0.5996

TABLE 7.1 (Contd.)

$\alpha \tan \delta / C_L$

Wings η	123	124	134	234	1234	Flat Plate
0.0000	0.2485	0.2409	0.2330	0.2225	0.1802	0.1927
0.1000	0.2368	0.2324	0.2282	0.2222	0.1911	0.1927
0.2000	0.2071	0.2097	0.2134	0.2183	0.2154	0.1927
0.3000	0.1739	0.1817	0.1910	0.2046	0.2303	0.1927
0.4000	0.1565	0.1617	0.1685	0.1805	0.2170	0.1927
0.5000	0.1707	0.1653	0.1603	0.1585	0.1796	0.1927
0.6000	0.2184	0.2018	0.1839	0.1646	0.1540	0.1927
0.7000	0.2734	0.2590	0.2419	0.2191	0.1883	0.1927
0.8000	0.2643	0.2743	0.2320	0.2838	0.2730	0.1927
0.9000	0.0542	0.0887	0.1233	0.1570	0.1910	0.1927
0.9500	-0.1925	-0.1722	-0.1509	-0.1274	-0.0986	0.1927
0.9950	-0.5356	-0.5680	-0.5993	-0.6278	-0.6579	0.1927
1.0000	-0.5823	-0.6239	-0.6646	-0.7105	-0.7443	0.1927

TABLE 7.1 (Contd.)

$\mathcal{C}(\eta)$

Wings η	12	13	14	23	24	34
0.0000	0.6381	0.6389	0.6395	0.6395	0.6396	0.6397
0.1000	0.6408	0.6392	0.6387	0.6373	0.6371	0.6365
0.2000	0.6468	0.6383	0.6359	0.6317	0.6302	0.6293
0.3000	0.6509	0.6369	0.6297	0.6230	0.6191	0.6160
0.4000	0.6447	0.6276	0.6173	0.6107	0.6038	0.5972
0.5000	0.6179	0.6043	0.5938	0.5909	0.5821	0.5725
0.6000	0.5593	0.5567	0.5511	0.5542	0.5473	0.5407
0.7000	0.4596	0.4721	0.4767	0.4846	0.4854	0.4873
0.8000	0.3157	0.3391	0.3547	0.3624	0.3740	0.3854
0.9000	0.1402	0.1594	0.1754	0.1784	0.1928	0.2067
0.9500	0.0555	0.0651	0.0739	0.0746	0.0830	0.0924
0.9950	0.0019	0.0023	0.0027	0.0027	0.0031	0.0032
1.0000	0.0000	0.0000	0.0000	0.0000	0.0000	0.0000

TABLE 7.1 (Contd.)

$f'(\eta)$

Wings η	123	124	134	234	1234	Flat Plate
0.0000	0.6829	0.6785	0.6749	0.6710	0.6461	0.6368
0.1000	0.6727	0.6697	0.6675	0.6657	0.6469	0.6334
0.2000	0.6462	0.6461	0.6470	0.6496	0.6455	0.6238
0.3000	0.6113	0.6129	0.6157	0.6214	0.6321	0.6073
0.4000	0.5774	0.5775	0.5785	0.5826	0.5995	0.5835
0.5000	0.5498	0.5457	0.5417	0.5392	0.5502	0.5513
0.6000	0.5240	0.5167	0.5085	0.4993	0.4973	0.5093
0.7000	0.4803	0.4760	0.4701	0.4610	0.4514	0.4546
0.8000	0.3843	0.3901	0.3944	0.3953	0.3926	0.3820
0.9000	0.2039	0.2162	0.2278	0.2381	0.2475	0.2775
0.9500	0.886	0.0965	0.1044	0.1118	0.1196	0.1988
0.9550	0.0034	0.0038	0.0042	0.0046	0.0050	0.0636
1.0000	0.0000	0.0000	0.0000	0.0000	0.0000	0.0000

TABLE 7.2 : GROSS PROPERTIES OF OPTIMAL CONICAL WINGS

$C_L = 0.1$, $a = 0.5$, $\tan\delta = 1.0$, $AR = 4.0$

Wings	C_D	L/D	e	α_0	ϵ_0	ϵ_2	ϵ_4	ϵ_6	ϵ_8
12	0.00134	74.56	1.6854	0.01568	-0.01568	-0.11709	0.58148	--	--
13	.00132	75.69	1.6602	.01698	-0.01698	-0.08765	--	0.64218	--
14	.00131	76.47	1.6433	.01764	-0.01764	-0.05772	--	--	0.77868
23	.00131	76.46	1.6436	0.01824	-0.01824	--	-0.57172	1.27449	--
24	.00130	77.03	1.6314	.01855	-0.01855	--	-0.28318	--	1.15973
34	.00129	77.26	1.6224	.01885	-0.01885	--	--	-1.25466	2.30337
123	.00129	77.28	1.6262	.02485	-0.02485	0.24342	-1.88103	2.58974	--
124	.00129	77.68	1.6178	.02409	-0.02409	0.17543	-0.98035	--	1.95084
134	.00128	77.99	1.6112	.02332	-0.02332	0.10043	--	-2.77598	4.01783
234	.00128	78.25	1.6060	.02225	-0.02225	--	-1.28706	-2.33394	6.61757
1234	.00127	78.48	1.6013	.01797	-0.01797	-0.24401	3.58514	-11.69602	10.13964
Flat Plate	.00124	80.76	1.5560	.01927	-0.01927	--	--	--	--

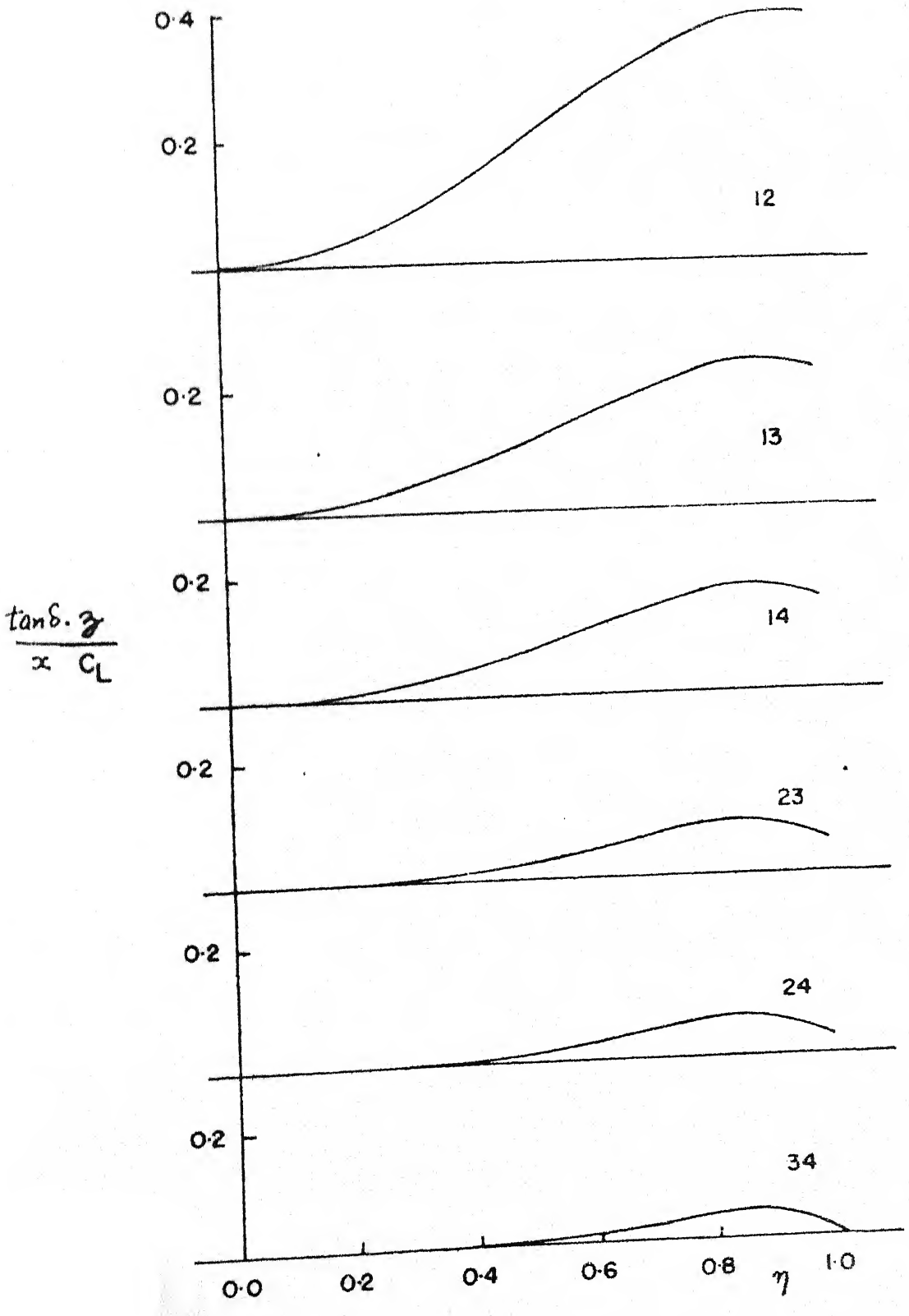

FIG. 7.2. OPTIMAL WING SHAPES. (a = 0·5)

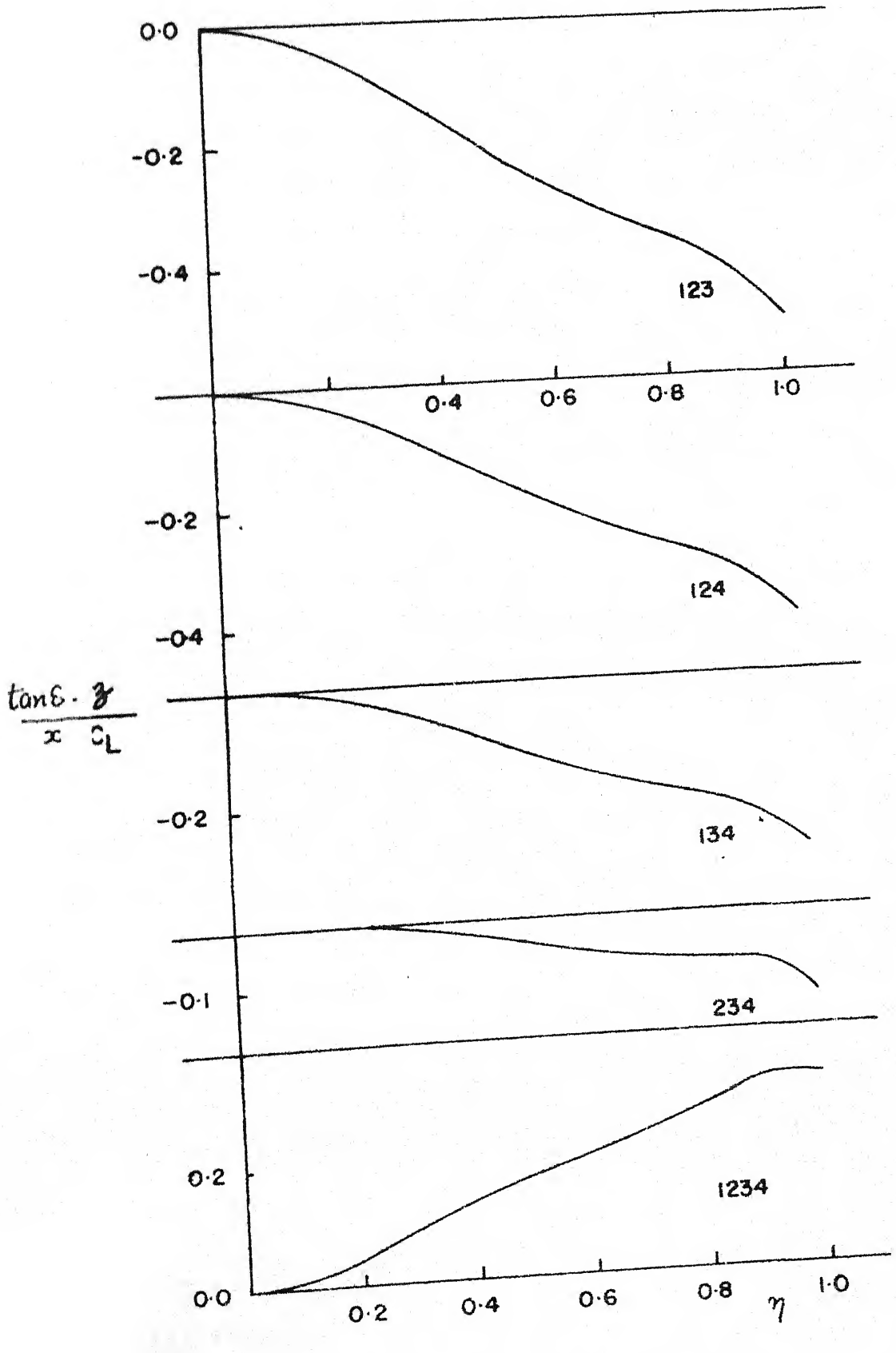

FIG. 7.2(CONTD). OPTIMAL WING SHAPES (a=0·5)

twist distribution, in either case, tends to flatten the wing. Surface wariness, apart from the leading edge droop, although discernible, is small. The number of waves increases with increasing number of basic twist distributions. All the shapes have leading edge droop which should help to smoothen the flow, and the outboard portions have a washout in incidence which should alleviate tip stall.

Table (7.2) shows that one may, with little effort, obtain drag coefficients quite close to the plane delta with suction and the optimal shapes in Fig. 7.2 show that these shapes are practically useful in the sense that they do not violate our notions of a good design in a real viscous flow. It is clear from Table (7.1) that use of higher order basic twists or combinations of larger number of twists in a design pushes the pressure peak outboard, increases the peak intensity and by acting on the forward facing drooped portion of the leading edge produces a thrust force that alleviates drag. In fact Table (7.2) shows that the suction force lost by prescribing an attachment line at the leading edge is admirably made up by the pressures acting on the droop, and drag values quite close to the plane delta wing with suction are attainable.

Another interesting feature of these designs is that for an even number of twist distributions the wing incidence

and the wing root pressure coefficient increases as higher order basic shapes are used. For odd number of combinations the opposite trend is true, Table (7.1). Further, unlike the works of Tsien and Holla, where marked variations in the optimal shapes may occur with changes in the design Mach number (or the slenderness parameter) the present designs show rather mild changes (data not presented). This may be taken to indicate that the off-design performance of our wings will be better, in the sense, that they do not show abrupt changes in behaviour, and hence are likely to be more useful in practice.

CHAPTER 8

DISCUSSIONS AND EXTENSIONS

8.1 Summary of Present Work

Several problems connected with the design of a delta wing using conical camber have been studied. Design methods have been studied and developed under equality and inequality constraints for obtaining minimum drag wings. These methods are illustrated for a conically cambered delta wing with subsonic leading edges in a supersonic stream, and carrying a polynomial twist distribution, each term of which is an even order term in the conical coordinate. An additional restriction is that the load at the leading edge is zero at the design condition. This is a practically useful condition since such wings are less prone to flow separation and the theoretical results are likely to be closer to the real situation. This way useful wing shapes have been obtained whose aerodynamic characteristics come close to the plane delta with leading edge suction.

The results of Chapters 4 and 6 are, however, not restricted to delta wings only, but may be applied to more general planforms and twist distributions in subsonic and supersonic flow. The results of the leading edge vortex phenomenon in Chapter 3 appear promising and with further refinements

may form a reliable method of predicting pressures, at least for the case of a plane delta wing at an incidence. It also includes compressibility effects.

In Chapter 7, the programming methods are illustrated by numerical examples for minimum drag wing designs subjected to realistic constraints. They are thus shown to be useful design tools.

8.2 Future Extensions

It would be of interest to obtain the low speed characteristics of the conical wings described in Chapter 2 and to see what kind of modifications they might need, if any. At low aspect ratios, the leading edge vortex phenomenon is to be expected. It is not yet clear how a twist distribution will affect the leading edge vortex growth and how it will interact with a thickness distribution. Experimental work in this area is definitely needed, not only to understand the phenomenon more clearly, but also to generate data for comparison with theory.

The programming techniques proposed in Chapter 6 have a natural extension to problems with non-linear constraints. Further the objective function need not be just the drag expression but some other criteria. For example, it may be the manufacturing cost, or it may be a combination of drag and manufacturing cost with each being given a certain weight

factor which would indicate their relative importance in the optimization decisions.

Several techniques are known for solving the general non-linear programming problem where the objective function and the constraints are allowed to be non-linear. Except under restrictive circumstances, none of these guarantee a global optimum solution. They generally give a local optimum which may or may not be the global optimum. In any case, it is more than likely that the solution would be useful or a different guess at the solution for the first iteration will give a result closer to expectations. The literature in this area is vast and rapidly growing, and remains a potential source for new optimization methods.

REFERENCES

1. Busemann, A.
   Aerodynamischer Auftrieb bei Uberschallgeschwindigkeit, Volta Congress, 328-360 (1935).

2. Brebner, G.G.
   Some Simple Conical Camber Shapes to Produce Low Lift Dependent Drag on a Slender Delta Wing ARC CP 428 (1957).

3. Cooke, J.C.
   Properties of a Two Parameter Family of Thin Conically Cambered Delta Wings by Slender Body Theory, ARC R&M 3249 (1960).

4. Jones, R.T.
   Properties of Low Aspect Ratio Pointed Wings at Speeds above and below the Speed of Sound, NACA Rept. 835 (1946).

5. Smith, J.H.B.
   The Properties of a Thin Conically Cambered Wing According to Slender Body Theory, ARC R&M 3135 (1958).

6. Smith, J.H.B. and Mangler, K.W.
   The use of Conical Camber to Produce Flow Attachment at the Leading Edge of a Delta Wing and to Minimize Lift Dependent Drag at Sonic and Supersonic Speeds, ARC R&M 3289 (1957).

7. Holla, V.S.
   Studies on Conically Cambered Wings, Ph.D. Thesis, IISc., Bangalore (1967).

8. Tsien, S.H.
   The Supersonic Conical Wing of Minimum Drag, J. Aero. Sci., 22, 805-817, (1955).

9. Weber, J.
   Design of Warped Slender Wings with Attachment Lines along the Leading Edge, ARC R&M 3406 (1957).

10. Bolton-Shaw, B.W.
    Nose Controls on Delta Wings at Supersonic Speeds, College of Aeronautics, Cranfield, Rept. 36 (1950).

11. Lance, G.N.
The Delta Wing in a Non-Uniform Supersonic Stream, Aero. Quart. 5, 55-72, (1954).

12. Lance, G.N.
The Lift of Twisted and Cambered Wings in Supersonic Flow, Aero. Quart. 6, 149-163 (1955).

13. Baldwin, B.S.
Triangular Wings Cambered and Twisted to Support Specified Distribution of Lift at Supersonic Speeds, NACA TN 1816 (1949).

14. Germain, P.
General Theory of Conical Flows and Its Application to Supersonic Aerodynamics (Translation), NACA TM 1354 (1955).

15. Multhopp, H.
A Unified Theory of Supersonic Wing FlowEmploying Conical Fields, RAE Rept. Aero. 2415 (1951).

16. Lagerstrom, P.A.
Linearized Supersonic Theory of Conical Wings, NACA TN 1685 (1948).

17. Carafoli, E.
High Speed Aerodynamics, Pergamon Press (1956).

18. Carafoli, E.
Wing Theory in Supersonic Flow Pergamon Press (1969).

19. Jones, R.T. and Cohen, D.
High Speed Wing Theory, Princeton Aeronautical Paperbacks, Princeton Univ. Press (1960).

20. Hayes, W.D.
Linearized Supersonic Flow, North American Aviation Co. Rept. AL-222 (1947).

21. Von Karman, T.
Supersonic Aerodynamics-Principles and Applications, J. Aero. Sci. 14, 373-409 (1947).

22. Puckett, A.
Supersonic Wave Drag of Thin Airfoils, J. Aero. Sci., 13, 475-484 (1946).

23. Stewart, H.J.
A review of Source Superposition and Conical Flow Methods in Supersonic Wing Theory, J. Aero. Sci., 23, 507-516, (1956).

24. Evvard, J.C.
Use of Source Distributions for Evaluating Theoretical Aerodynamics of Thin Finite Wings at Supersonic Speeds, NACA Rept. 951 (1950).

25. Krasilshchikova, E.A.
Uchenya Zapiski 154, Mekhanika 4, 181-239 (1951), Transl. NACA TM 1383 (1956).

26. Etkin, B. and Woodward, F.A.
Lift Distribution on Supersonic Wings with Subsonic Leading Edges and Arbitrary Angle of Attack Distribution, J. Aero. Sc. 21, 783-785 (1954).

27. Puckett, A.E. and Stewart, H.J.
Aerodynamic Performance of Delta Wings at Supersonic Speeds, J. Aero. Sci., 19, (1952).

28. Munk, M.M.
Minimum Induced Drag of Aerofoils, NACA Rept. 121 (1921).

29. Munk, M.M.
The Reversal Theorem of Linearized Supersonic Airfoil Theory, J. App. Physics, 21, 159-161 (1950).

30. Jones, R.T.
The Minimum Drag of Thin Wings in Frictionless Flow, J. Aero. Sci., 18, 75-81 (1951).

31. Jones, R.T.
Theoretical Determination of the Minimum Drag of Airfoils at Supersonic Speeds, J. Aero. Sci. 19, 813-822 (1952).

32. Graham. E.W.
A Drag Reduction Method of Wings of Fixed Planform, J. Aero. Sci., 19, 823-825, (1952).

33. Rodriguez, A.M., Lagerstrom, P.A. and Graham, E.W.
Theorems Concerning the Drag Reduction of Wings of Fixed Planform, J. Aero. Sci, 21, 1-8, (1954).

34. Cohen, D.
The Warping of Triangular Wings for Minimum Drag at Supersonic Speeds, J. Aero. Sci., 24, 67-68 (1957).

35. Ginzel, I and Multhopp, H.
Wings with Minimum Drag Due to Lift in Supersonic Flow, J. Aero. Sci. 27, 13-20 (1960).

36. Ursell, F. and Ward, G.N.
On Some General Theorems in the Linearized Theory of Compressible Flow, Quart, J. Mech. and App.Match. 3, Pt. 3, 326-348 (1950).

37. Flax, A.H.
General Reverse Flow and Variational Theorems in Lifting Surface Theory, J. Aero. Sci., 19, 361-374, (1952).

38. Flax, A.H.
The Reverse Flow Theorem for Non-stationary Flow, J. Aero. Sci., 19, 352-353, (1952).

39. Flax, A.H.
Reverse Flow and Variational Theorems for Lifting Surfaces in Non-stationary Compressible Flow, J. Aero. Sci., 20, 120-126 (1953).

40. Bollay, W.
A Theory for Rectangular Wings of Small Aspect Ratio J. Aero. Sci., 4, 294-296 (1937).

41. Gersten, K.
Non-Linear Wing Theory Specially for Aircraft Wing with Small Aspect Ratio (in German), Sonderabdruck aus 'Ingenieur Archiv', 30-431-452 (1961).

42. Betz, A.
Applied Aerfoil Theory, Article in Aerodynamics Theory, IV, edited by W.G. Durand (1935).

43. Eranshaw, P.D.
An Experimental Investigation of the Structure of a Leading Edge Vortex, ARC R&M 3281 (1962).

44. Lambourne, N.C. and Bryer, D.W.
The Bursting of Leading Edge Vortices - Some Observations and Discussion of the Phenomenon, ARC R&M 3282 (1962).

45. Hall, M.G.
The Structure of Concentrated Vortex Cores, Progress in Aeronautical Sciences, 7, 53-110, (1966).

46. Hall, M.G.
Vortex Breakdown, Annual Review of Fluid Mechanics, 4, (1972).

47. Kirkpatrick, D.L.I.
Experimental Demonstration of the Similarity of Leading Edge Vortices above Slender Wings in Subsonic Conical Flow, Sonderdruck aus dem Jahrbuch 1967 der WGLR, 223-231, (1967).

48. Legendre, R.
Ecoulement an Voissinage de la Pointe Avan D'une Aile a Farte Fleche Aux Incidences Moyennes, La Recherche Aeronautique, Nov-Dec. (1952) and Jan-Feb. (1953).

49. Adams, M.C.
Le Leading Edge Separation from Delta Wings at Supersonic Speeds, J. Aero. Sci., 20, 430, (1953).

50. Edwards, R.H.
Leading Edge Separation from Delta Wings, J. Aero. Sci., 21, 134-135, (1954).

51. Brown, C.E. and Michael, W.H.
Effect of Leading Edge Separation on the Lift of a Delta Wing, J. Aero. Sci., 21, 690-694, (1954).

52. Mangler, K.W. and Smith, J.H.B.
A Theory of the Flow Past a Slender Delta Wing with Leading Edge Separation, Proc. Roy. Soc., London (A) 251, 200-217, (1959).

53. Smith, J.H.B.
Improved Calculations of Leading Edge Separation from Slender Delta Wings, RAE TR 66070 (1966).

54. Kuchemann, D.
Non-Linear Lifting Surface Theory for Wings of Small aspect Ratio with Edge Separation, RAE Rept. 2540, (1955).

55. Squire, L.C.
The Estimation of the Non-Linear Lift of Delta Wings at Supersonic Speeds, J. Roy. Aero. Soc., 67, 476-480 (1963).

56. Polhamus, E.
Predictions of Vortex Lift Characteristics by a Leading Edge Suction Analogy, J. Aircraft, 8, 193-199, (1971).

57. Hadley, G.
Linear Programming, Addision-Wesley Pub. Co., Inc., (1965).

58. Hadley, G.
Non-Linear and Dynamic Programming, Addison-Wesley Pub. Co., Inc., (1964).

59. Kuhn, H.W. and Tucker, A.W.
Non-linear Programming, Proceedings of the Second Berkeley Symposium on Mathematical Statistics and Probability, 481-492, (1951).

60. Beale, E.M.L.
Mathematical Programming in Practice, Sir Issac Pitman and Sons, Ltd., (1968).

61. Ashley, H. and Landahl, M.
Aerodynamics of Wings and Bodies, Addison-Wesley Pub. Co., Inc., (1965).

62. Rogers, E.W.E. and Berry, C.J.
Experiments at M = 1.41 on Elliptic Cones with Subsonic Leading Edges, ARC R&M 3042, (1955).

63. Rogers, E.W.E., Quincey, V.G. and Callinan, J.
Experiments at M = 1.41 on a Thin Conically Cambered Elliptic Cone of 30° Semi-Vertex Angle, ARC R&M 3306, (1961).

64. Squire, L.C., Jones, J.G. and Stanbrook, A.
An Experimental Investigation of Some Plane and Cambered 60° Delta Wings at Mach Numbers for 0.7 to 2.0, ARC R&M 3305 (1961).

65. Jones, R.T.
Three Dimensional Wings of Minimum Pressure Drag, Article in Theory of Optimum Aerodynamic Shapes, Edited by A. Miele, Academic Press, 125-134, (1965).

66. Grant, F.C.
The Proper Combination of Lift Loadings for Least Drag on a Supersonic Wing, NACA TN 3533, (1955).

67. Laidlaw, W.R. and Hsu, P.T.
A Semi-empirical Method for Determining Delta Wing Pressure Distributions in an Incompressible Flow, J. Aero. Sci., 21, 854-856, (1954).

68. Truckenbrodt, E.
Jahrbuch 1953 der Wiss Ges. F. Luftfahrt.

69. Maskell, E.
The Flow Separation in Three Dimensions, ARC 18063 (1955).